PEOPLE'S DEMOCRATIC REPUBLIC OF ALGERIA
MINISTRY OF HIGHER EDUCATION AND SCIENTIFIC RESEARCH
IBN KHALDOUN UNIVERSITY – TIARET
FACULTY OF MATHEMATICS AND COMPUTING
COMPUTER DEPARTMENT

THESIS

Presented by :

BAYA REDOUANE
CHEKARI MOKHTAR

For the graduation of :

MASTER

Specialty : Network and Telecommunications

On the subject

Simulation Study of HEMT performance for high frequency applications

---

Publicly presented on 29/11/2020 in Tiaret in front of the composed jury:

Mr. CHENINE Abdelkader	M.A.A	IBN-KHALDOUN Tiaret University	President
Mrs. KERMAS Nawel	M.A.A	IBN-KHALDOUN Tiaret University	Supervisor
Mr. DAOUED Bachir	M.A.A	IBN-KHALDOUN Tiaret University	Examiner

Année Universitaire : 2019 -2020

ACKNOWLEDGEMENT

First of all, we thank Almighty God for giving us the courage, patience, moral and physical strength to be able to do this work.

Our gratitude goes to Mrs. KERMAS Nawel for her guidance, advice and the availability she has shown us to enable us to carry out this work.

We would like to express our sincere thanks to Mr. CHENINE Abdelkader who accepted to chair the defense jury, for everything he could teach us; may he find here the expression of our deep and sincere gratitude. Mr. DAOUED Bachir for doing us the honor of accepting to review this work.

We address our thanks to all the professors, for their advice and their critiques which guided our reflections during our research, and we also thank all our colleagues and friends of the computer science department of the Ibn Khaldoun University in Tiaret.

We would like to express our deep gratitudes to our parents who have supported us throughout our project, as well as all the family, friends for their indefictable support.

Finally, we thank all those who helped us directly or indirectly in the development of this work.

DEDICATION

From the bottom of our hearts, we dedicate this work to:

Our families, BAYA and CHEKARI, in particular our parents. This thesis would not have seen the light of day without their encouragement over the years.

To all of our brothers and sisters.

To our colleagues CHARFAOUI Younes, BOURBIE Ismail, AZAZEN Walid, DOULAMI Hami, AIT HAMOU Khaled, BENGHALEM Aziz and ALEM Habib who helped us throughout our studies.

To my friends KHIATI Houssam, BOUDJENANE Howari and to the people who have always believed in us.

TABLE OF CONTENTS

Chapter I: gallium-nitride technology. 2
I.1 Introduction 2
I.1. 1 Brief History of GaN Technology 4
I.2 Basic properties of GaN 6
I.2.1 Crystal structure 6
I.2.1.1 Wurtzite structure 7
I.2.1.2 Zinc blende structure 8
I.2.2 Electronic band structure 10
I.3 Application Areas of GaN 11
I.3.1 Optical applications 12
I.3.2 Electronic applications 14
I.4 Gallium Nitride Power Semiconductors Market 18
I.5 The III-nitride alloys 20
I.6 $Al_xGa_{1-x}N$/GaN heterostructure 22
I.7 Summary 24
Chapter II: AlGaN/GaN High Electron Mobility Transistors (HEMTs) 26
II.1 Introduction 26
II.2 High Electron Mobility Transistors (HEMTs) 27
II.2.1 Background 27
II.2.2 $Al_xGa_{1-x}N$/GaN HEMTs structure 28
II.3 Growth techniques and substrates choice 30
II.3.1 Silicon Carbide Substrates (SiC) 32
II.3.2 Sapphire Substrates *(Al_2O_3)* 33
II.3.3 Silicon Substrates (Si) 33
II.4 HEMTs operation 34
II.4.1 DC characteristics 34
II.4.2 Degradation of HEMT performance 36
II.4.2.1 Off-State Stress 37

II.4.2.2High-Temperature Stress 38
II.4.3 Breakdown mechanisms 39
II.5 Summary 41
Chapter III: Simulation results and discussion 42
III.1 Introduction 42
III.2 About Matlab 42
III.3 Model definition 44
III.4 HEMT Device Structure 50
III.5 Resultats and Discussion 51
III.5.1 Simulation resultats 51
III.6 Conclusion 55
IV Conclusion and future work prospects 56
IV.1 General Conclusion 56
IV.2 Future work prospects 57
REFERENCES 58

LIST OF FIGURES

Figure I. 1 Possible crystal structures for III-V semiconductors. 6
Figure I. 2 Wurtzite structure of GaN. 7
Figure I. 3 Gallium and nitrogen polarities in hexagonal GaN [23]. 8
Figure I. 4 Zinc blende structure of GaN. 9
Figure I. 5 Second neighbors in the wurtzite and zinc blende structures [28]. 9
Figure I. 6 GaN cubic Zinc Blende (left) and hexagonal Wurtzite (right) structure and their Brillouin zones. 10
Figure I. 7 GaN würtzite band structure along high symmetry lines in the Brillouin zone.... 11
Figure I. 8 Bandgap energy versus lattice constant for various semiconductors including the wide-bandgap materials SiC and GaN with its alloys. 12
Figure I. 9 GaN-based micro-electronics applications. 15
Figure I. 10 GaN semiconductor devices market by product. 19
Figure I. 11 Global market revenue forecast for GaN and SiC power semiconductors. 20
Figure I. 12 The III-nitride from periodic table. 21
Figure I. 13 Bandgap energies as a function of lattice parameter of group III-nitrides.......... 22
Figure I. 14 Band diagram for the AlGaN/GaN heterostructure, with Ef the Fermi level energy, EC the conduction band energy and ΦB the Schottky barrier height. ΔEC is the energy difference between the AlGaN and GaN respective conduction bands [52]. 23
Figure I. 15 The structure of a typical AlGaN/GaN HEMT with an insulation layer and 2DEG charges. 24

Figure II. 1 Structure of an AlGaN/GaN HEMT transistor. 28
Figure II. 2 Structure for HEMT simulation (left) and theoretical ideal characteristics Ids-Vds for an AlGaN/GaN HEMT t different gate Voltage (right). 35
Figure II. 3 HEMT DC characteristics. 36
Figure II. 4 Different conditions of typical DC characteristic curves. (a) Transfer characteristic and transconductanceharacteristics; (b) gate leakage current. 38
Figure II. 5 Different conditions of typical DC characteristic curves. (a) Transfer characteristic and transconductanceharacteristics; (b) gate leakage current. 38

Figure III. 1 Matlab logo (left), creation of Matlab logo (right). 43
Figure III. 2 Matlab example program. 44
Figure III. 3 Heterostructure interface and energy band profile of an AlGaN/GaN HEMT. . 45
Figure III. 4 Cross sectional view of AlxGa1-xN/GaN nanostructures HEMTs using for simulation. 51
Figure III. 5 Electrical characteristics of AlxGa1-xN/GaN HEMTs for different gate-to-source voltage. 52

Figure III. 6 Electrical characteristics of AlxGa1-xN/GaN HEMTs for different gate width Z. 53
Figure III. 7 Electrical characteristics of AlxGa1-xN/GaN HEMTs for different Barrier layer thickness. 54
Figure III. 8 Electrical characteristics of AlxGa1-xN/GaN HEMTs for different spacer layer thickness. 54

LISTE OF TABLES

Table I. 1 The parameters of GaN and AlN lattice at 300K. 7
Table I. 2 Parameters of the ideal and real wurtzite structure of GaN [21]. 8
Table I. 3 Band gap width for GaN and AlN, in hexagonal and cubic phases. 11
Table I. 4 Application areas of gan materials and energy saving 17

Table II. 1 Crystallographic characteristics of the substrates used for the growth. 31
Table II. 2 Characteristics of semiconductors. 31

Table III. 1 List of Symbols. 44

LIST OF ABBREVIATIONS AND SYMBOLS

GaN	Gallium Nitride
AlGaN	Aluminium Gallium Nitride
SiC	Silicon Carbide
Si	Silicon
CB	Conduction Band
VB	Valence Band
EF	Electric Field
BV	Breakdown Voltage
2DEG	Two Dimentional Electron Gas
WBG	Wide Band Gap
CTE	Coefficient of Thermal Expansion
FP	Field Plate
HEMT	High Eelctron Mobility Transistor
FET	Field Effect Transistor
MOSFET	Metal Oxide Semiconductor Field Effect Transistor
MESFET	MEtal-Semiconductor Field Effect Transistor
MBE	Molecular Beam Epitaxially
MOCVD	Metal-Organic Chemical Vapor Deposition
LDMOS	Laterally diffused metal oxide semiconductor

RF	Radio Frequency
PAE	Power Added Efficiency
SBH	Schottky Barrier Height
Cg	Gate Capacitance
Cgd	Gate-Drain Capacitance
Lg	Gate Length
μn	Electron Mobility
ns	Charge Density at AlGaN/GaN Interface
Cg	Gate Capacitance
Ron	On-state Resistance
ro	Output Impedance

GENERAL INTRODUCTION

Silicon based semiconductor devices are rapidly approaching the theoretical limit of operation and are becoming unsuitable for future communication and military requirements. Wide band gap semiconductors have greater prospects compared to Silicon based devices. The wide band gap material system shows higher breakdown voltage, lower leakage, higher saturation velocity, larger thermal conductivity and better thermal stability suitable for high-power, high-speed, and high-temperature operations of the devices. A new generation of high speed – high frequency devices is required to meet current and future communication and military needs [1].

$Al_xGa_{1-x}N$ /GaN based HEMTs are becoming one among the favorite choices for future high-frequency, high-power, high temperature electronics applications. This can be attributed to the excellent physical properties such as a wide band gap (more than 3.4 eV), a high critical field for breakdown, and a good thermal conductivity of these nitride based heterostructure. The most interesting feature of these devices is the presence of a high mobility, two-dimensional electron gas (2DEG) with a sheet density of the order of 1013 cm^{-2} at the AlGaN/GaN interface. This phenomenon is attributed to the strong piezoelectric as well as spontaneous polarization effects in these nitride based devices, allowing an efficient, gate-controlled charge transport between the source and drain electrodes of the device [2].

It is very important to understand the fundamental properties of these devices, including the mechanism responsible for the formation of the 2DEG, and how this is influenced by a large number of different physical properties such as polarity, alloy composition, strain, thickness, and doping of the AlxGa1-xN barrier [2].

Chapter I
Gallium-Nitride technology

Chapter I: gallium-nitride technology.

I.1 Introduction

Semiconductors are materials which have a conductivity between conductors (generally metals) and nonconductors or insulators (such as most ceramics). Semiconductors can be pure elements, such as silicon or germanium, or compounds such as gallium nitride or cadmium selenide. In a process called doping, small amounts of impurities are added to pure semiconductors causing large changes in the conductivity of the material [3].

Due to their role in the fabrication of electronic devices, semiconductors are an important part of our lives. Imagine life without electronic devices. There would be no radios, no TV's, no computers, no video games, and poor medical diagnostic equipment. Although many electronic devices could be made using vacuum tube technology, the developments in semiconductor technology during the past 50 years have made electronic devices smaller, faster, and more reliable. Think for a minute of all the encounters you have with electronic devices. How many of the following have you seen or used in the last twenty-four hours? Each has important components that have been manufactured with electronic materials [3].

A compound semiconductor is a semiconductor compound composed of chemical elements of at least two different species. These semiconductors typically form in periodic table groups 13–15 (old groups III–V), for example of elements from the Boron group (old group III, boron, aluminium, gallium, indium) and from group 15 (old group V, nitride, phosphorus, arsenic, antimony, bismuth). The range of possible formulae is quite broad because these elements can form binary two elements, e.g. gallium nitride (GaN), ternary three elements, e.g. aluminium gallium nitride (AlGaN) alloys [4].

Gallium nitride (GaN) is a binary III-V direct bandgap semiconductor commonly used in light-emitting diodes since the 1990s. GaN has very high chemical resistance to corrosive environments. Strong bond existing between Ga and nitrogen is responsible for the corrosion resistance properties the compound. The compound is a very hard material that has a Wurtzite crystal structure. Its wide band gap of 3.4 eV affords it special properties for applications in optoelectronic, high-power and high-frequency devices. For example, GaN is the substrate which

makes violet (405 nm) laser diodes possible, without use of nonlinear optical frequency-doubling. Gallium nitride is prepared by the reaction of Ga_2O_3 with NH_3 at elevated temperatures of the order of 1000°C [4].

It can be also prepared by the chemical vapor deposition of organometallic compounds containing Ga and nitrogen atoms. Corrosive acids and alkaline environments do not have any effect on GaN phase as revealed by X-ray diffraction and electrical conductivity measurements. Its sensitivity to ionizing radiation is low (like other group III nitrides), making it a suitable material for solar cell arrays for satellites. Military and space applications could also benefit as devices have shown stability in radiation environments. Because GaN transistors can operate at much higher temperatures and work at much higher voltages than gallium arsenide (GaAs) transistors, they make ideal power amplifiers at microwave frequencies. In addition, GaN offers promising characteristics for THz devices [5].

GaN with a high crystalline quality can be obtained by depositing a buffer layer at low temperatures. Such high-quality GaN led to the discovery of p-type GaN, p-n junction blue/UV-LEDs and room-temperature stimulated emission (essential for laser action). This has led to the commercialization of high-performance blue LEDs and long-lifetime violet-laser diodes, and to the development of nitride-based devices such as UV detectors and high-speed field-effect transistors [5].

In this chapter we present the basic properties of gallium-nitride (GaN) technology, namely their different crystal and electronic band structures. Also GaN application areas and its material system and the power semiconductors market.

I.1.1 Brief History of GaN Technology

GaN materials has a longer history than it is generally perceived, GaN materials in the early development stage were powder forms prepared mostly by chemists. The studies were focused on the synthesis processes of nitrides of various metallic compounds, also including boron nitride (BN) and aluminum nitride (AlN), and their fundamental properties. The synthesis of GaN materials is traced back to the 1930s [6].

The material system of interest in this thesis is the wide-bandgap III-V compound semiconductor gallium nitride (GaN). GaN was first synthesized by Juza and Hahn in the 1930s by passing ammonia (NH3) over liquid gallium (Ga) at elevated temperatures. This method resulted in a powder consisting of small needles and platelets. Their purpose was to investigate the crystal structure and lattice constant of GaN [6].

In 1968, Maruska and Tietjen were the first to try the hydride vapor phase epitaxy (HVPE) approach to grow centimeter-sized GaN layers on sapphire substrates. In a traditional HVPE reactor the group III element such as Ga is transported as the monochloride. For example, gallium chloride (GaCl) is generated in *situ* by passing hydrochloric acid vapor (HCl (g)) over liquid Ga. The group V element such as nitrogen (N) is transported as the hydride. Sapphire was chosen as substrate material because it is a robust material that is not reactive with ammonia. To date, sapphire has remained a very popular substrate for heteroepitaxial GaN growth. The early HVPE GaN films were grown at temperatures below 600°C to prevent decomposition. In 1969, Maruska realized that in an ammonia environment at temperatures above 600°C GaN growth actually would occur instead of decomposition. He increased the growth temperature to 850°C, the temperature typically used for gallium arsenide (GaAs), and obtained the first single crystalline GaN film. The film quality could even be improved by increasing the temperature to 950°C. All GaN films grown at that time showed very high electron concentrations (1020 cm^{-3}) even without intentional doping. The responsible n-type donors were believed to be nitrogen vacancies, a concept that has caused a lot of controversy over the years. Eventually oxygen has been proposed as the responsible donor. Oxygen with its six valence electrons on an N site (N has five valence electrons) would be a single donor [7].

In the late 1970s, GaN research ceased virtually everywhere because of the continuing difficulties encountered with the growth of high quality films needed for device development. Remaining issues were the choice and availability of a suitable substrate, how to control the very high intrinsic n-type conductivity, and difficulties with obtaining conducting p-type GaN films. In

1982 only a handful of papers were published world-wide on this material system. It was the perseverance of Isamu Akasaki that eventually resulted in obtaining conducting p-type GaN films in 1989 [7].

In 1986, a milestone was achieved when Amano et al. reported highly improved surface morphology, and optical and electrical properties of GaN films grown by metal organic chemical vapor deposition (MOCVD) on sapphire substrates through the use of a low-temperature (600°C) aluminum nitride (AlN) nucleation layer. This layer is grown between the sapphire substrate and the bulk GaN film, which is typically grown at 1050°C. In 1991, Shuji Nakamura of the Japanese company Nichia Chemical Industries extended this concept with the introduction of a low-temperature (450−600°C) GaN nucleation layer. The reason for this was that the large lattice mismatch between the low-temperature AlN nucleation layer and the following GaN film could cause defect generation and that the use of a low-temperature GaN nucleation layer would prevent this. To date, MOCVD is the workhorse for the growth of GaN and related materials[8].

In the early 1990s, gallium nitride (GaN) was deemed an excellent, next generation, semiconductor material for high power/high frequency transistors based on the material parameters of bandgap, electron mobility, and saturated electron velocity. The lack of bulk GaN source material led to the need for GaN growth on mismatched substrates such as Si, SiC and sapphire, but fundamental material development controlled the pace of maturation of GaN technology for both electronic and optoelectronic applications. The development of GaN for RF electronics was significantly aided by the intense development that occurred in the race to first production of blue and, eventually, white light-emitting diodes (LEDs). Ultimately, advancements in the growth of device-grade aluminum gallium nitride (AlGaN)/GaN heterostructures culminated in the demonstration of record power density RF amplifiers [8].

I.2 Basic properties of GaN

I.2.1 Crystal structure

Most III-V materials crystallize in two forms: zinc blende (ZnS) or sphalerite (cubic), and hexagonal or wurtzite. This arrangement consists of two face-centered cubic sub-arrays, one consisting of an element III and the other of an element V.

The phase which is thermodynamically the most stable for element III nitrides is wurtzite phase with hexagonal symmetry. The type of structure depends on the orientation of the substrate. To obtain a hexagonal phase, a hexagonal substrate oriented [0001] is used, for example Al_2O_3 or SiC. The wurtzite phase is characterized by two subnets compact hexagonal offset along the c axis. The first sub-network is formed by atoms nitrogen and the second by the gallium atoms which occupy half of the tetrahedral sites. The mesh is described by two mesh parameters a and c; a corresponds to the side of the hexagon in the plane (0001) and c at the height of the cell along axis [0001] (it corresponds to two atomic monolayers (MC)). In an ideal wurtzite structure, the c/a ratio is $\sqrt{8/3} \approx$ 1.633. In real structures, this report makes it possible to obtain an indication of deviation from the ideal wurtzite structure. Quantum wells which are studied in the context of this thesis are made from GaN layers inserted between $Al_xGa_{1-x}N$ layers. It is therefore necessary to know the properties of these two materials [9].

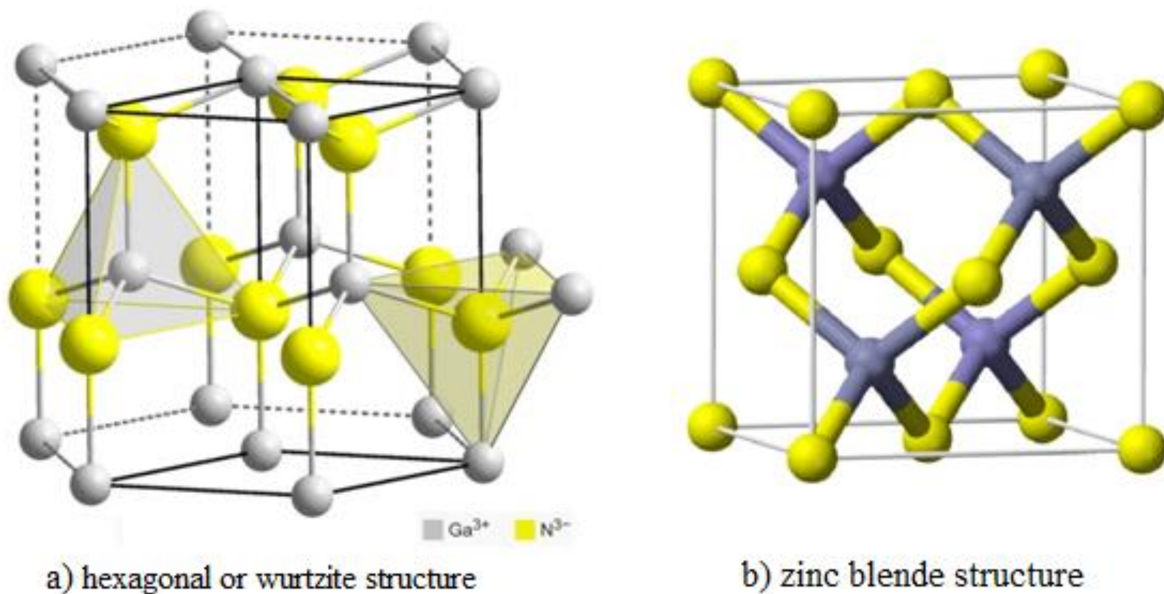

Figure I. 1 Possible crystal structures for III-V semiconductors.

	GaN	AlN
a (Å)	3.189	3.112
c (Å)	5.185	4.982
c/a	1.626	1.600

Table I. 1 The parameters of GaN and AlN lattice at 300K.

I.2.1.1 Wurtzite structure

In the wurtzite structure (Figure 2), nitrogen atoms form a compact hexagonal stacking. Gallium atoms occupy half of the sites tetrahedral. There are two GaN form units per cell. This structure is characterized by the mesh parameters a and c, but also by the parameter u = l / c, where l is the Ga-N bond length according to c. For GaN single crystals produced by synthesis under high temperature and high nitrogen pressure, a and c vary between 3.1881 and 3.1890Å respectively; and between 5.1664 and 5.1856Å, exclusively depending on the concentration of free electrons in the crystal. For GaN, a and c thin films may vary slightly depending on the purity chemical, free electron concentration and stresses [10].

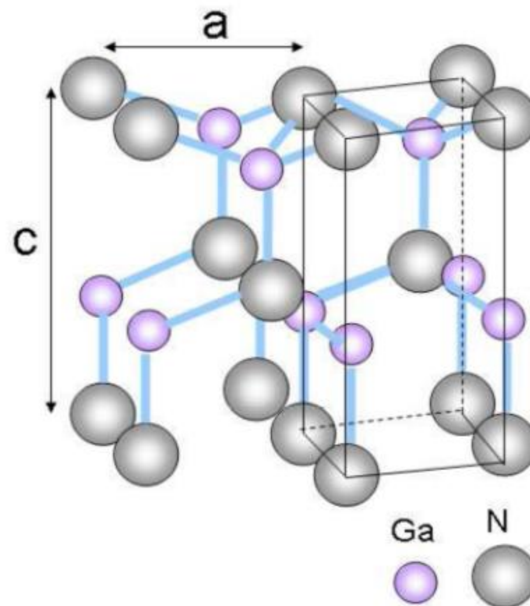

Figure I. 2 Wurtzite structure of GaN.

The structure of gallium nitride deviates only slightly from the wurtzite structure ideal (Table 2). The gallium atoms are therefore in a very little distorted tetrahedral environment. Wurtzite

structure gallium nitride crystals adopt the most often a plate geometry, with the faces perpendicular to the c axis, or in prisms, whose axis of growth is the c axis [10].

GaN wurtzite	c/a	u
Ideal structure	1.633	0.376
Real structure	1.627	0.377

Table I. 2 Parameters of the ideal and real wurtzite structure of GaN [11].

The wurtzite structure is not symmetrical with respect to the (0001) plane, so we speak of polarity. Indeed, the directions [0001] and [$000\bar{1}$] are not equivalent. For nitride gallium, there are two possible arrangements of the gallium and nitrogen atoms during the growth. In the case where the GaN oriented bond points towards the surface, we say that we have a gallium polarity (Figure 3). Otherwise, we have a nitrogen polarity. It should be noted that the polarity of a layer does not predict the nature of the atoms on the surface. For example, a layer with gallium polarity can end with gallium atoms as well as with nitrogen atoms on the surface [12].

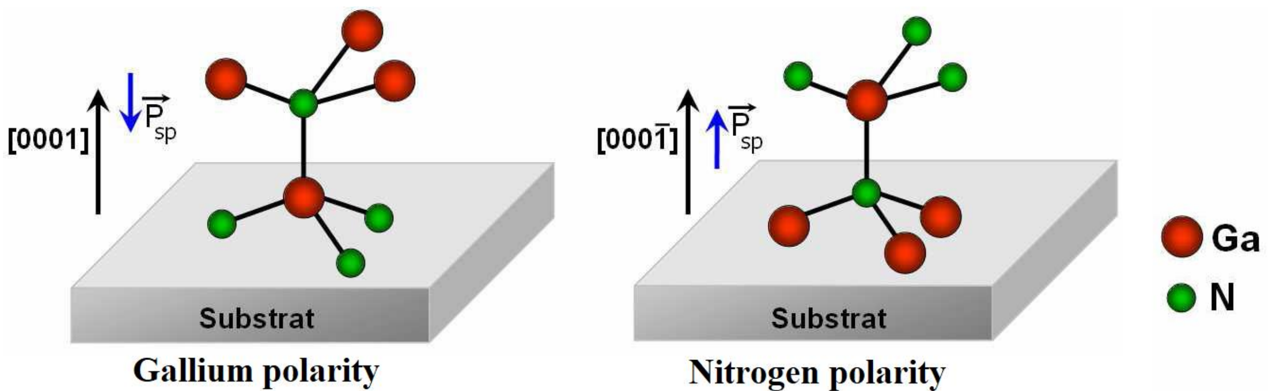

Figure I. 3 Gallium and nitrogen polarities in hexagonal GaN [12].

I.2.1.2 Zinc blende structure

In the zinc blende structure (Figure 4), the nitrogen atoms form a face-centered cubic stack in which the gallium atoms occupy half of the tetrahedral sites. This structure is characterized by the mesh parameter a [13].

The parameter observed varies between 4.51 and 4.52Å depending on the synthesis method used. Since this phase is metastable, its synthesis requires precise control of the experimental

parameters. The ammonothermal synthesis of pulverulent cubic GaN requires mastery of the experimental conditions (temperature, mineralizer: nature and concentration, etc.). In the case of the preparation of thin films, a substrate generally of cubic structure and specifically oriented (in order to disadvantage the formation of the hexagonal phase) is additionally necessary to stabilize the cubic phase. For example, the following substrates are used: MgO (100), Si (100), β-SiC (3C-SiC) (100), GaAs (001) or even Al_2O_3 (0001) [14].

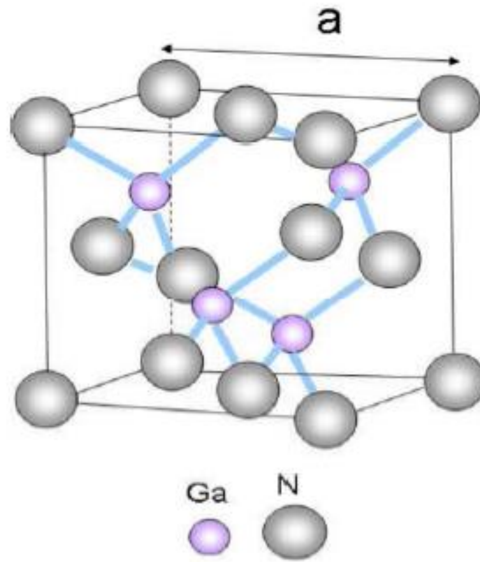

Figure I. 4 Zinc blende structure of GaN.

As we have just seen, the two structures differ only in terms of the stacking sequence of the crystalline planes (Figure 5). The crystallographic entourage of atoms differs only from the third neighbor.

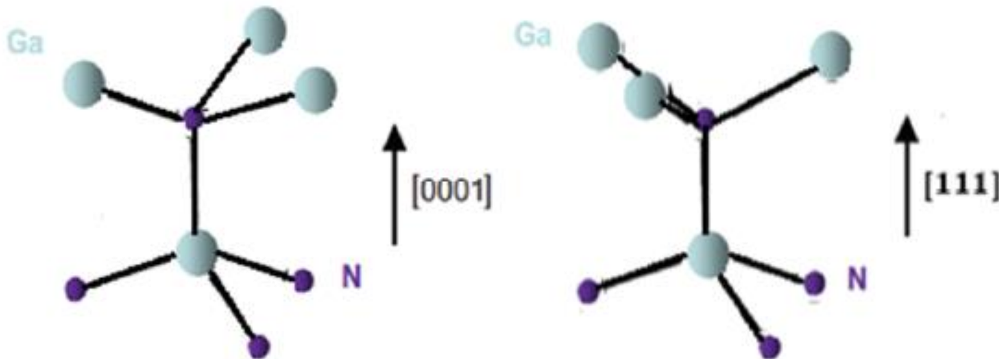

Figure I. 5 Second neighbors in the wurtzite and zinc blende structures [14].

I.2.2 Electronic band structure

To study the excitonic and electronic properties of a semiconductor, it is important to know the band structure of this material. GaN is a semiconductor presenting a direct band gap, which means that the conduction band minimum (Ec) and the valence band maximum (Ev) are at an almost identical value on the diagram representing the energy E relatively to the wave vector k. For GaN, this point is located at the Γ point, center of the Brillouin zone (k = 0). The first Brillouin zones and the band structures in the major direction are represented in (Figure 6) [15].

Hexagonal and cubic structures have a band gap of 3.43eV and 3.20eV respectively at 300K.

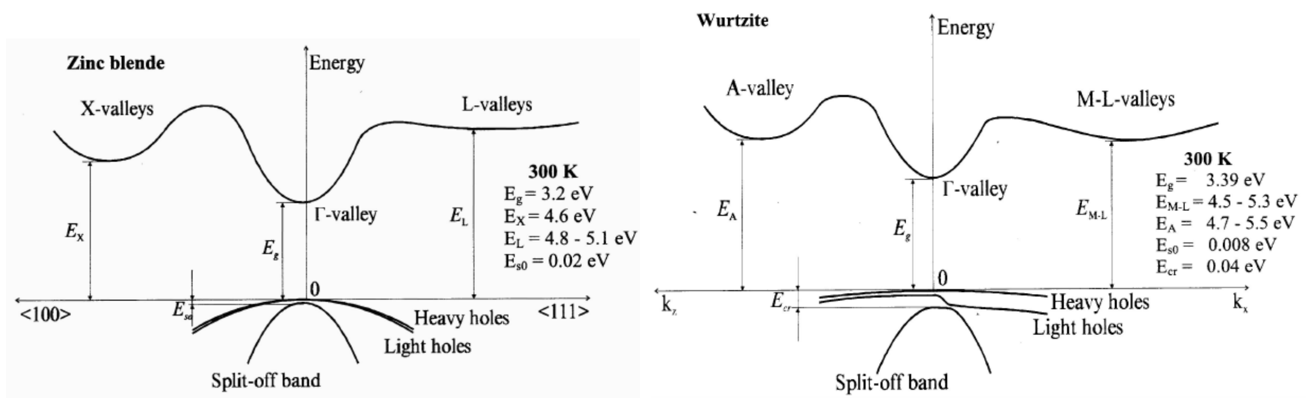

Figure I. 6 GaN cubic Zinc Blende (left) and hexagonal Wurtzite (right) structure and their Brillouin zones.

And (Figure 7) shows the band diagram of GaN würtzite along lines of high symmetry of the irreducible Brillouin zone calculated by Empirical pseudopotential method. This diagram shows the nature of the direct gap of GaN würtzite. The minimum of the conduction band and the maximum of the valence band are located in the center of the Brillouin area. At 300K, the generally accepted gap width is around 3.4eV [15].

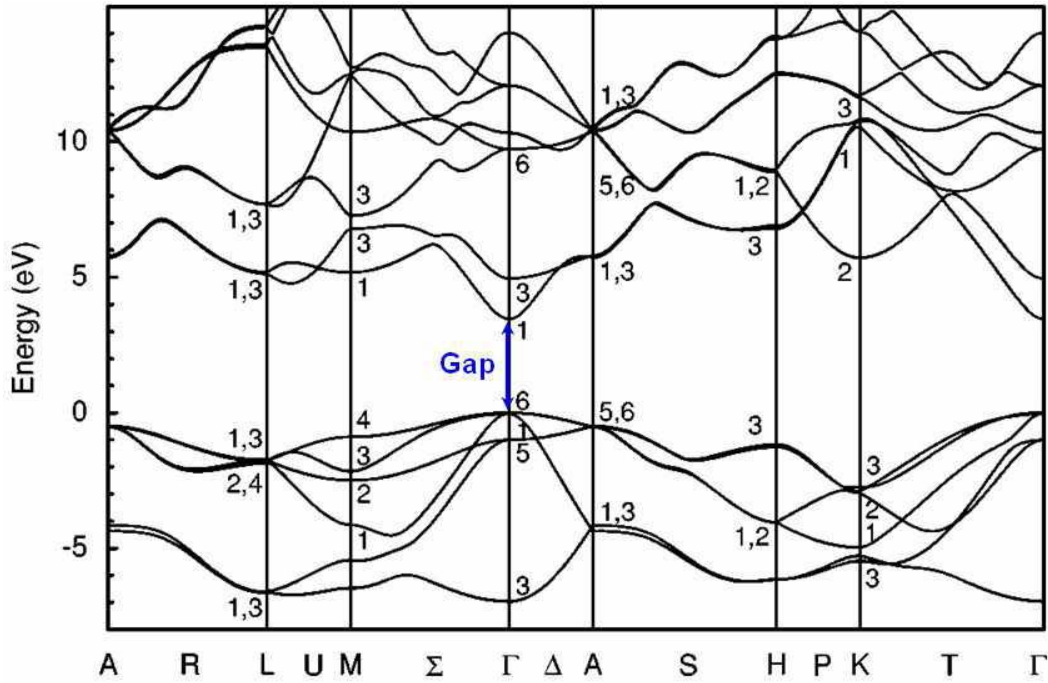

Figure I. 7 GaN würtzite band structure along high symmetry lines in the Brillouin zone.

(Table 3) represents the widths of the forbidden bands of GaN and AlN binary nitrides considered as "acquired" in hexagonal (wurtzite) phase and in cubic (zinc blende) phase at low temperature.

	Gap à 2K
GaN (Hex)	3.504 eV
GaN (Cub)	3.272 eV
AlN (Hex)	6.2 eV
AlN (Cub)	5.34 eV

Table I. 3 Band gap width for GaN and AlN, in hexagonal and cubic phases.

I.3 Application Areas of GaN

The direct bandgap of GaN and its alloys enables the material to be used for both optical and electronic applications. At 300 K the bandgap of GaN is 3.44 eV which corresponds to a wavelength

in the near ultra violet (UV) region of the optical spectrum. Figure 1.1 shows a plot of the bandgap energy versus lattice constant in combination with the visible optical spectrum for various semiconductors including the wide-bandgap materials SiC, GaN and its alloys indium nitride (InN) and aluminum nitride (AlN). It can be seen that the $Al_xIn_yGa_{1-x-y}N$ alloys cover bandgap energies from 1.9 eV to 6.2 eV, which correspond to wavelengths ranging from red to deep UV [16].

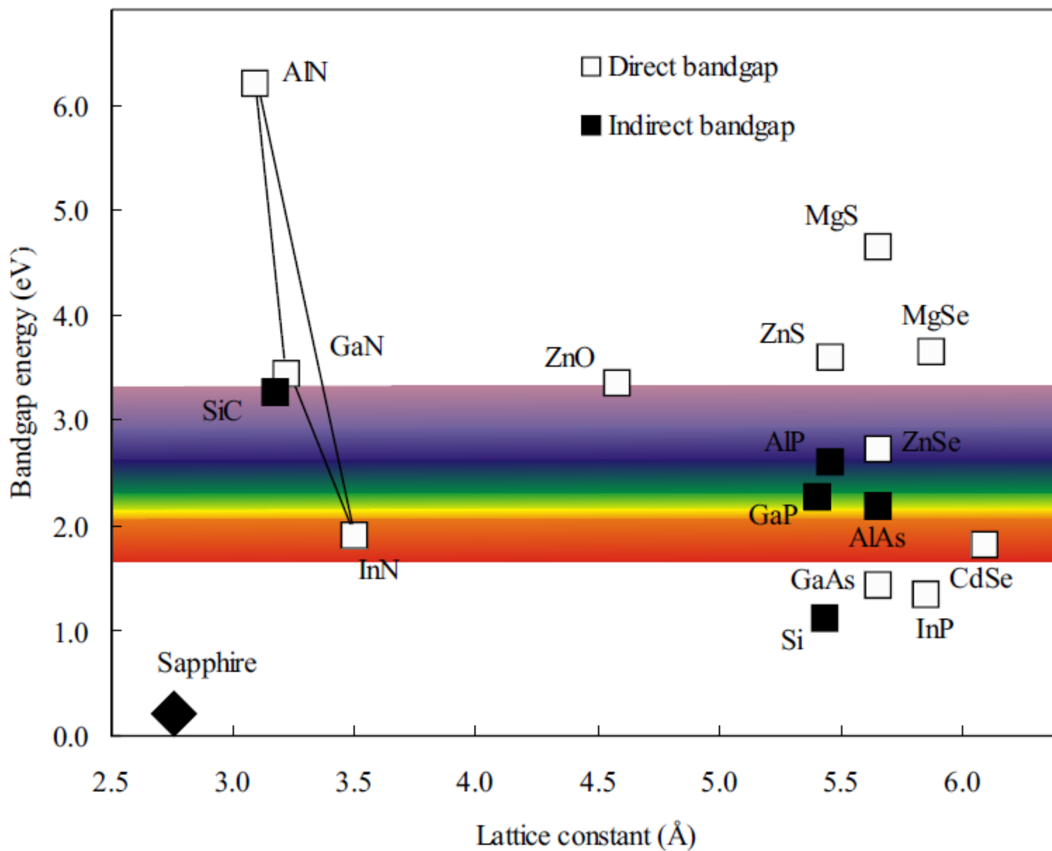

Figure I. 8 Bandgap energy versus lattice constant for various semiconductors including the wide-bandgap materials SiC and GaN with its alloys.

I.3.1 Optical applications

In 1968 James Tietjen, working at the Materials Research Division of the Radio Corporation of America (RCA), came up with the idea to develop a flat television that could be hung on the wall like a painting. A full color image can be created combining red, green, and blue pixels in the display. Red and green LEDs were available using gallium arsenide phosphide ($GaAs_{1-x}P_x$) and gallium phosphide nitride (GaP:N) materials, respectively. All that was missing to realise a flat LED-based television set was a bright blue LED. These devices became available using either SiC or II-VI compounds such as zinc oxide (ZnO). However, because of their indirect bandgap SiC LEDs were

not very efficient. The devices based on II-VI compounds mainly suffered from much too short lifetimes for commercial applications. Hence these devices could not be used in the envisioned display application [16].

LED applications

The main economical benefits of LED-based lighting are low power requirement, high efficiency, and long lifetime. In addition, solid-state design renders LEDs impervious to electrical and mechanical shock, vibration, frequent switching and environmental extremes. Several major markets are being addressed with these newly developed solid-state light sources. Automobile exterior lighting has been moving rapidly to incorporate transparent-substrate $Al_xIn_yGa_{1-x-y}P$ technology into high-mount braking lights and into the full amber and redorange taillight assembly. Full-color, outdoor, changeable message signs and full-motion video displays have been adopting $Al_xIn_yGa_{1-x-y}N$ and $Al_xIn_yGa_{1-x-y}P$ technologies and will continue to proliferate as costs are reduced. Traffic-signal applications have begun to incorporate red AlInGaP and AlGaAs LEDs for traffic lights and are moving toward incorporating amber and blue-green LEDs to produce a completely LED-based signal head. All of these markets are rapidly expanding and will provide enormous growth opportunities in the future. By using multiple LEDs, an LED cluster lamp continues to provide light even if one or more emitters fail unlike when the filament breaks in an incandescent bulb. Taking also into account an average life span of more than 100,000 hours (approximately 11 years), LEDs operate reliably year after year and are an excellent replacement for incandescent bulbs in hard-to-reach places and environments that depend on reliable lighting (e.g. hospitals, airports) [13]. Furthermore, colored lenses or filters are not needed since LEDs emit colored light that is determined by the composition of the semiconductor material comprising the diode. As LEDs are an energy-efficient light source and are virtually maintenance free, the cost savings are substantial. Other important GaN-based LED applications are backlighting (cell phones, PDAs), white light (flashlights, car head lights), general lighting (interior and exterior), water purification systems, and medical (sensors, surgical goggles) [17].

Laser applications

Infra-red AlGaAs-based and red AlInGaP-based laser diodes (LDs), such as those in today’s CD and DVD systems, have been around for decades. To increase the storage capacity on a CD, the pit size must be made smaller. A shorter wavelength LD is required to focus onto the smaller pit size. The current generation of DVD systems uses a LD with an emission wavelength of 650 nm. In the

last few years the market for DVD systems has increased rapidly. However, the majority of these systems is read-only and is based on a 5 mW AlInGaP LD emitting at 650 nm. For further advances in the market recordable DVD was an obvious necessity. This required higher output power from the 650 nm LD (typically 30 - 40 mW). To also achieve faster read/write speeds even higher powers are required.

GaN-based blue-violet LDs with an emission wavelength of 405 nm will be the cornerstone of next-generation DVD player-recorders and optical high-density data-storage systems for computers. Using these components it is already possible to write huge amounts of data (27 GB) on a single-layer 12 cm DVD disk which is almost six times the storage capacity possible with ordinary red LDs. This is enough to store more than two hours of high-definition (HD) video or 13 hours of standard-definition (SD) video [17].

I.3.2 Electronic applications

With respect to electronics, GaN is an excellent option for high-power/high-temperature microwave applications because of its high electric breakdown field (3 MV/cm) and high electron saturation velocity (1.5 x 107 cm/s). The former is a result of the wide bandgap (3.44 eV at RT) and enables the application of high supply voltages, which is one of the two requirements for high-power device performance. In addition, the wide bandgap allows the material to withstand high operating temperatures (300°C – 500°C). A big advantage of GaN over SiC is the possibility to grow heterostructures, e.g. AlGaN/GaN. The resulting two-dimensional electron gas (2DEG) at the AlGaN/GaN heterojunction serves as the conductive channel. Large drain currents (> 1 A/mm), which are the second requirement for a power device, can be achieved because of the high electron sheet densities (1 x 1013 cm^{-2}) and mobilities (1500 - 2000 cm^2/Vs). These material properties clearly indicate why GaN is a serious candidate for next-generation microwave high-power/high-temperature applications. (Figure 9) shows an overview of GaNbased micro-electronic applications [18].

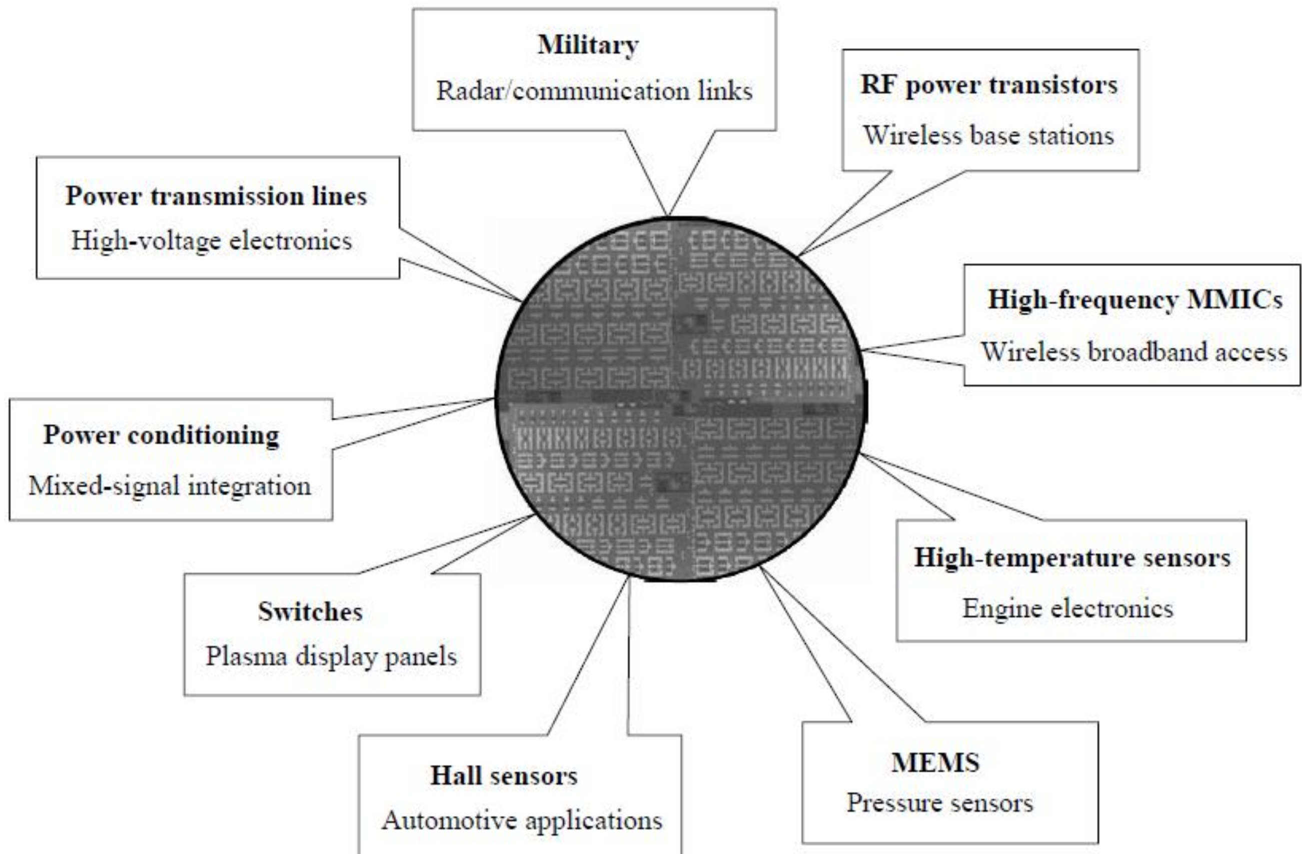

Figure I. 9 GaN-based micro-electronics applications.

Military applications

Despite the superior material properties and expected advances in device and system performance, the driving force behind research towards GaN-based microwave high-power/hightemperature electronics over the last decade has been almost exclusively military in nature. The main reason for this is the enormous costs that are involved with the early stages of GaN electronic device research. Several European countries, including France, Germany, United Kingdom, Italy, Spain, Sweden, and the Netherlands have defense oriented research programs, some of which are joint efforts such as the Swedish - Dutch SiC and GaN program (period: 2000 - 2005) and the new very big European GaN program KORRIGAN (Key Organization for Research on Integrated Circuits in GaN Technology) (period: 2005 - 2009). The frontiers of academic and military research and the commercialization of GaN-based electronics however are mainly in the US and to a lesser extent in Japan. US and Japanese research programs towards military microwave systems have been and continue to be heavily funded by the respective Departments of Defense (DoD). The US's Defense Advanced Research Projects Agency (DARPA) has granted a huge GaN

program, total investment up to $144.5 million, with a triple-pronged approach to speed up the development of GaN-based microelectronics and assure a rapid transition into military systems. Former research programs have focused on achieving hero values with respect to current densities and output power densities at microwave frequencies in order to prove the high expectations. The new programs however start for the basics (material growth, etching, contacts) and move through the stage of discrete devices to the eventual goal of GaN-based microwave monolithic integrated circuits (MMICs). The focus now is on understanding the physical reasons behind device failures and the development of physical models to predict performance in order to increase reproducibility and reliability. In general, defense research programs focus on the development of GaN technology for use in components such as surface radars, broadband seekers, jammers, battlefield communication, satellite communication links, transmit/receive modules, broadband high-power amplifiers (HPAs), and low noise amplifiers (LNAs). The frequencies of interest for these applications range from 2 GHz - 40 GHz [19].

Commercial applications

Commercial GaN-based applications are on the verge of their breakthrough. The first products will most probably be high-efficiency and high-linearity power amplifiers for base-stations, which power 3G wireless broadband cellular networks in the so-called S-band (2 GHz - 4 GHz). The US-based company RF Micro Devices (RFMD), the biggest player in this field, announced that it has sampled 100 W GaN amplifiers to customers early 2005. Competition can be expected from Japanese companies Fujitsu, Matsushita Electric, and OKI Electric. Other high-volume commercial applications in which GaN-based electronics could lead to significant performance enhancement and cost reduction are high-frequency MMICs (wireless broadband communication links), hybrid electric vehicles (DC-AC conversion), hightemperature electronics (automotive, energy production), switches (plasma display panels, low-frequency high-power switching), high-voltage power rectifiers (inverter modules), microelectro- mechanical systems, MEMS (pressure sensors), and Hall sensors (automotive applications) [19].

Current hybrid electric vehicle (HEV) platforms, which use silicon-based power electronics, are faced with two major challenges: size and weight. In addition to traditional cars containing internal combustion engines (ICEs), HEVs must also accommodate power electronics, energy storage, and an electric motor in the predefined volume of the automobile platform. The HEV’s motor drive, a power-electronics component that converts stored energy into an alternating-current

(AC) source needed to operate the electric motor, is one of the main contributors to the system's size and weight. Typically, HEV motor drives use silicon insulatedgate bipolar transistors (IGBTs) for the primary switching element, with Si p-i-n diodes as the fly-back diode, configured in a module designed to control three-phase motors. The module is positioned inside the engine compartment as close to the electric motor as possible to minimize parasitic inductance and reduce cabling weight. However, like all silicon devices they are limited to junction temperatures of 150oC - 175oC. Controlling the junction temperature of the Si electronics in the engine compartment's harsh environment requires large heat sinks and liquid cooling, but both these solutions are costly and difficult to integrate into the volume available within the engine compartment. The temperature limitations inherent to Si technology mean that state-of-the-art Si electronic components cannot meet the demands of HEV platforms to produce smaller, lighter, and cheaper electrical systems [19].

Motor Drive applications

Application areas	Application effect
Electric vehicles	Reducing energy consumption by 20%
High speed railway	Saving energy more than 10%, while reducing the power system volume
Household appliances	Energy saving 50%
Industrial motor	Energy saving 30% ～ 50%
Aerospace	Reducing equipment loss 30% to 50%, Increasing operating frequency by 3 times, Reducing the volume of components 2/3
Smart Grid	Reducing power loss by 50%, while increasing power efficiency by more than 30%
Solar energy generation	Reducing the photoelectric conversion loss by more than 25%
Wind power generation	Increasing the efficiency of 20%
Large capacity communication	Significantly improving signal transmission efficiency, safety and stability

Table I. 4 Application areas of gan materials and energy saving

As listed in (Table 4), GaN material has a broad application prospect, and is one of the effective ways to realize energy saving and consumption reduction in the world. In this part, the application and research status of GaN power devices are summarized. Especially, the devices were used in motor drive system. Meanwhile, the existing problems and the direction of solution are discussed [19].

I.4 Gallium Nitride Power Semiconductors Market

The allowable costs depend to a great extent on the application area. For commercial applications it is eminent that cost reduction is the driving force for any material system to survive. To service the wide range of applications, GaN technology must be cost-competitive throughout the range of frequencies presently addressed by Si LDMOS, GaAs MESFET, and InP pHFET. To meet strict cost requirements the technology must be based on a large diameter, low cost substrate material such as Si or HVPE grown bulk GaN. Cost reduction on a system level is feasible because of GaN's high-temperature operation that eliminates the need of bulky cooling units. In addition, GaN devices do not require as much off-chip circuit protection as GaAs transistors hence elimination of these circuits leads to weight and cost savings. Furthermore, the ability of GaN transistors to produce higher power densities not only allows the use of smaller and fewer transistors in total but also the reduction or even elimination of costly linearization circuitry necessary for high-bandwidth wireless systems. It should be noted that these cost requirements stand in strong contrast with military applications which are mainly performance driven [20].

In 2004, the worldwide GaN device market, which was overwhelmingly dominated by LED sales, was worth $3.2 billion. For the year 2009, Strategies Unlimited estimates this value to be $7.2 billion. It is expected that optical applications will still dominate sales and account for 83% of this amount, leaving 17% to electronic applications such as microwave high-power amplifiers (HPAs) [20].

The global gallium nitride semiconductor devices market size was valued at USD 974.9 million in 2016. The market is expected to experience significant growth over the next eight years, owing to the accelerating demand for power electronics that consume less power and are energy efficient. GaN-based semiconductors possess dynamic electrical and chemical properties, such as high-voltage breakdown and saturation velocity that make them the appropriate choice for use in a variety of switching devices [21].

Manufacturers are focused on making improvements to the GaN technology and most of the technological advancements were made from 2010 to 2016. In 2010, the first gallium nitride power device was released by International Rectifier. In 2012, the first 6 inch GaN-on-Si Epiwafers were introduced in the market. The prominent industry players are engaged in undertaking collaborations and strategic partnerships for developing and improving the GaN technology [21].

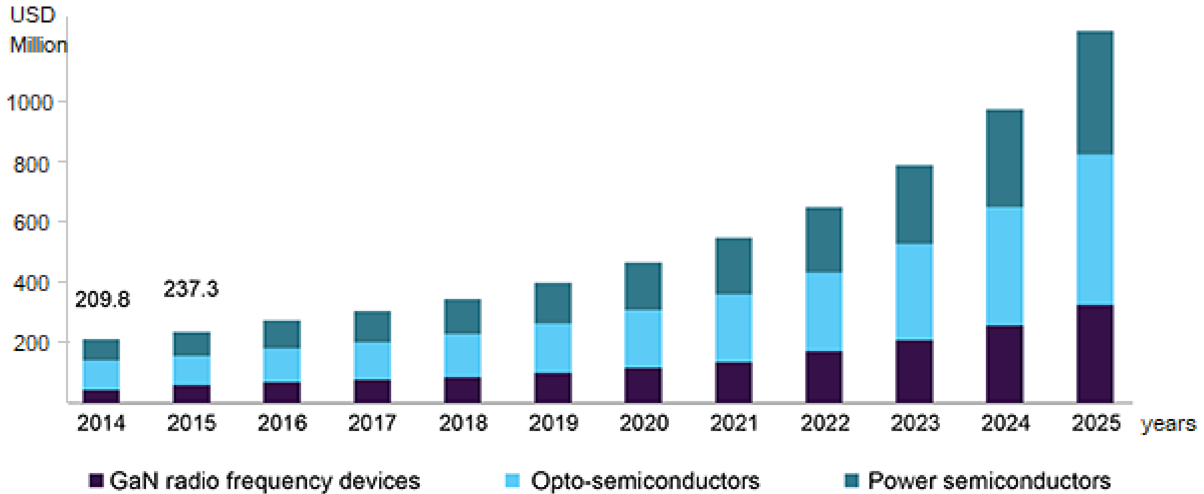

Figure I. 10 GaN semiconductor devices market by product.

Most industry experts anticipate gallium nitride to substitute silicon, owing to its high efficiency and low power consumption capabilities. It is also expected to be apt material for manufacturing power electronic devices. Moreover, gallium nitride-based transistors provide high thermal conduction, large electric field, and higher breakdown voltage with a wide ban. The transistors are functional at high power density & high switch frequency and are more efficient as compared to silicon devices. The GaN technology is expected to witness significant demand in the healthcare sector. The hospitals are observed taking the help of robots equipped with gallium nitride components to conduct delicate surgeries. Furthermore, scanning equipment, such as sonograms, MRI, and miniaturized x-ray machines, makes use of GaN-based semiconductor components, owing to their precise positioning capabilities that are helpful in performing surgeries [22].

The emerging market for silicon carbide (SiC) and gallium nitride (GaN) power semiconductors is forecast to pass $1 billion in 2021, energized by demand from hybrid & electric vehicles, power supplies, and photovoltaic (PV) inverters. Worldwide revenue from sales of SiC and GaN power semiconductors is projected to rise to $854 million by the end of 2020, up from just $571 million in 2018, according to Omdia's SiC & GaN Power Semiconductors Report – 2020. Market revenue is expected to increase at a double-digit annual rate for the next decade, passing $5 billion by 2029. These long-term market projection totals are about $1 billion lower than those in last year's edition of this report. This is because demand for almost all applications has slowed since 2018. Moreover, device average prices fell in 2019. A note a caution: The equipment forecasts used to create this year's forecast all date from 2019, and do not take account of the impact of the COVID-19 pandemic [22].

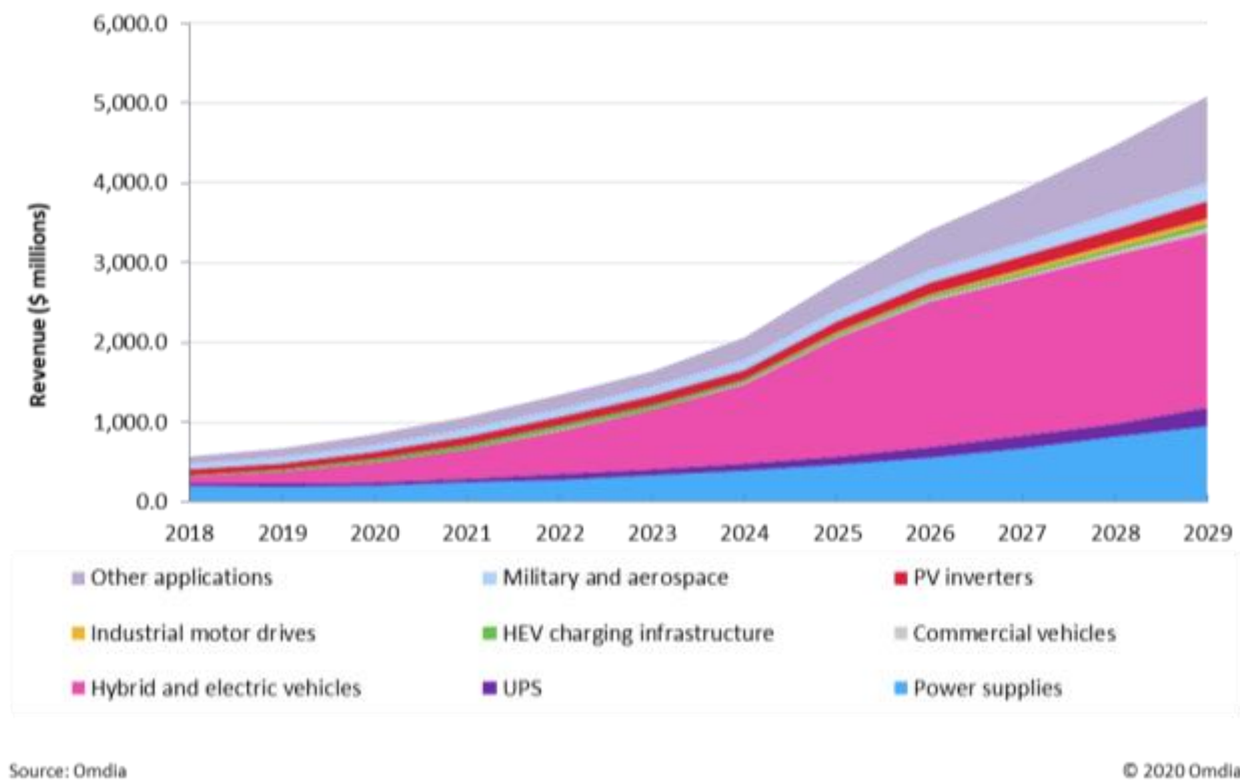

Figure I. 11 Global market revenue forecast for GaN and SiC power semiconductors.

I.5 The III-nitride alloys

Group III-nitride semiconductors, including AlN, GaN, InN, and their alloys form a group of materials with high perspectives because of their good properties, such as: high iconicity, low compressibility, high melting point, high thermal conductivity, chemical inertness, high breakdown voltages, and ability to sustain high-temperature and high-power operation. They are direct bandgap materials and can crystallize in both wurtzite and zinc blende polytypes [23].

(Figure 12) shows a periodic table extract of group III-IV-V

Figure I. 12 The III-nitride from periodic table.

III-Nitrides alloys (GaN, InGaN, AlGaN and AlInGaN) are widely used for several applications, such as High Electron Mobility Transistors (HEMT), solar cells, light emitting devices. These alloys show a bandgap tunable with composition, covering the whole visible spectrum; however, these materials suffer from the presence of structural defects emerging from strain and thermal relaxation phenomena. We study transport properties, optical spectra, and electrical properties at macro and nano-scale and quantum confinement effects in order to clarify the role of material properties on device behavior [23].

The III-Nitrides materials system has impacted energy efficiency on the worldwide scale through its application to blue light-emitting diodes (LEDs). This impact on technology and society was recognized by the award of the 2014 Nobel Prize in Physics to Isamu Akasaki, Hiroshi Amano, and Shuji Nakamura. The binary nitrides cover a wide range of direct band gap energies with energy gap tunable by alloy composition ranging from 0.65 eV (InN) to 6.0 eV (AlN). However, the large mismatch in lattice constants between the nitrides and their substrates results in highly strained heterostructures with ternary alloys. This strain can lead to defect formation, reduced material quality, and polarization-related electric fields in basal plane growth [24].

(Figure 13) shows band gap energy versus lattice constant for III–N semiconductors, considering the following bowing parameters: 1.6, 0.7, and 3.4 for $In_xGa_{1-x}N$, $Al_xGa_{1-x}N$, and $In_xAl_{1-x}N$, respectively [24].

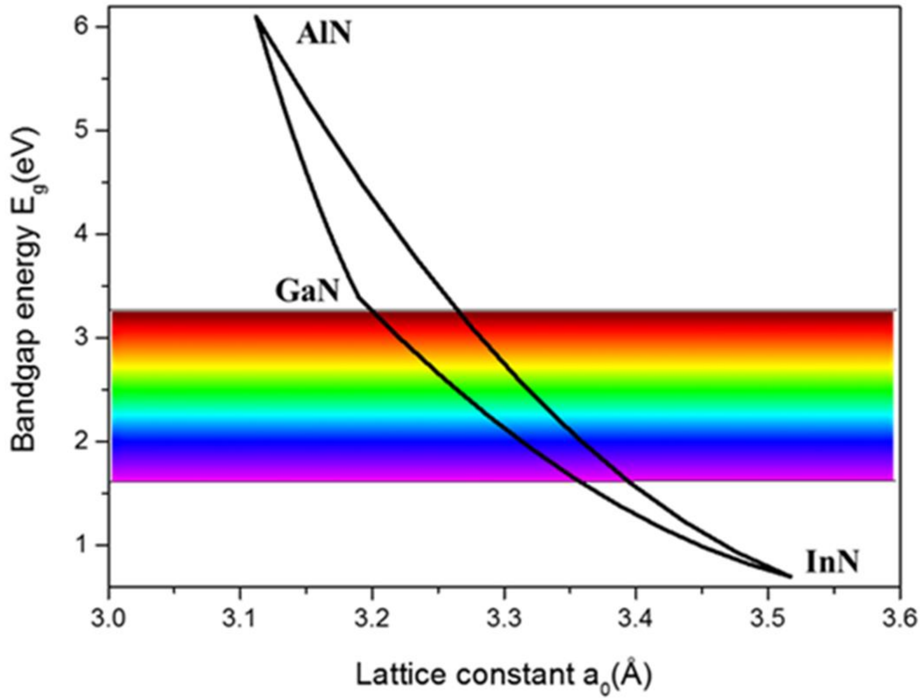

Figure I. 13 Bandgap energies as a function of lattice parameter of group III-nitrides.

Of particular interest can be $In_xAl_{1-x}N$, due to the wide range of bandgap energies accessible, but also because it can be grown lattice-matched to GaN at a composition of 18% In, suitable for strain-free barrier and capping layer. Despites these perspectives, not many reports exist on the growth of $In_xAl_{1-x}N$, a lot of problems arising from the high immiscibility in the range $0.1 < x < 0.9$ and lattice mismatch between AlN and InN, of ~ 13%. These problems can be easily surpassed by using non-equilibrium growth techniques such as MSE, and full-composition range was demonstrated [25].

I.6 $Al_xGa_{1-x}N$/GaN heterostructure

AlGaN/GaN heterostructures are of high research and industrial interest for the production of high electron mobility transistors (HEMT) utilizing the two-dimensional electron gas (2DEG) induced at the interface due to polarization effects. In the current work, the effect of AlGaN thickness on 2DEG formation is under discussion. In particular, ultrathin layers of AlGaN (between 2–12 nm thick) are grown on top of GaN. Composition of these layers is studied and variations of surface potential are mapped using Kelvin probe force microscopy (KPFM) to see the evolution of the 2DEG formation in relation to layer thickness and stoichiometry. The obtained results allow

concluding about critical thickness of AlGaN layer for the formation of continuous 2DEG at the AlGaN/GaN interface [26].

As stated earlier, one of the major applications in power devices for which GaN is considered among the best materials is the creation of HEMT structures. Compared to traditional MESFET (Modulation Electron Surface Field Effect Transistor), the HEMT is able to bypass the problem of electron transportation in highly doped environment, which presents many restrictive phenomenons regarding electronic performances, especially for mobility. The main principle behind the high mobility transistor is to create a bidimensional electron gas (2DEG) using an AlGaN/GaN heterojunction, which band diagram is represented in (Figure 14) [26].

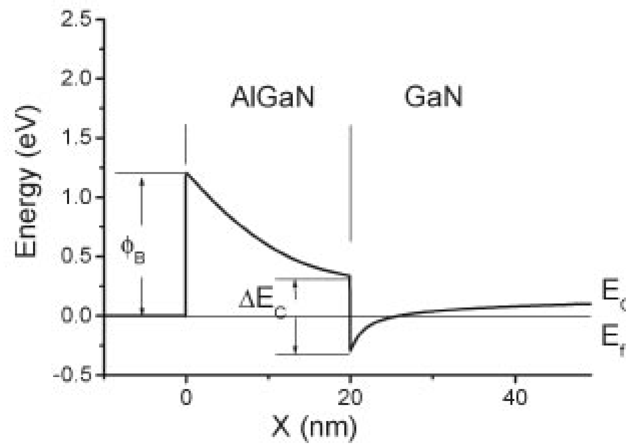

Figure I. 14 Band diagram for the AlGaN/GaN heterostructure, with Ef the Fermi level energy, EC the conduction band energy and ΦB the Schottky barrier height. ΔEC is the energy difference between the AlGaN and GaN respective conduction bands [26].

By choosing the right material, we can create a localized potential drop of the conduction band below the Fermi level and confine the carriers in a quantum well. The resulting potential and associated band diagram are thus directly related to the band gap of each semiconductor and their respective doping levels. The electron exchange between the two materials allows Fermi levels alignment and, as in a PN junction, a space charge appears [27].

The resulting well in GaN is a high electron density region with an excellent mobility, since it is free of any impurity. Electrons can move freely between source and drain along the heterojunction in a bidimensional space. Despite the restrictive aspect of the 2DEG, electron concentration in such structures can achieve very high levels, up to $2x10^{13}$ cm^{-2}. It is important to notice that this value is referenced as a unit of surface and not volume [27].

The HEMT structure represented in (Figure 15) presents a typical heterojunction between the GaN buffer layer and the AlGaN barrier. In this transistor, gate modulation is achieved by applying negative voltages which allows depleting more or less the bidimensional channel between the gate and the drain. This kind of operation is referred to as depletion transistor or normally-on.

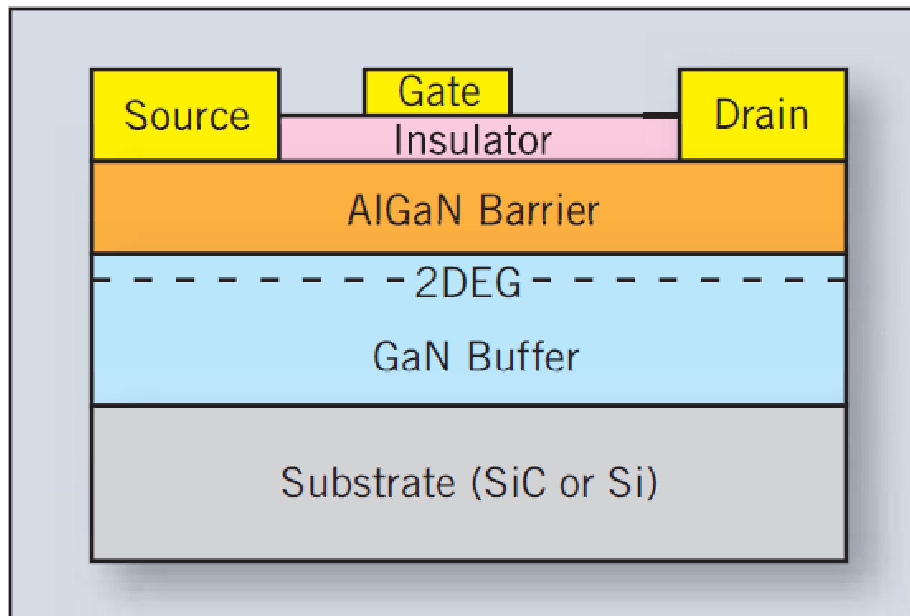

Figure I. 15 The structure of a typical AlGaN/GaN HEMT with an insulation layer and 2DEG charges.

I.7 Summary

In this first chapter, we gived a brief history of GaN technology that has a longer history than it is generally perceived, we first analyzed the basic propreties of GaN namely their different crystal and electronic band structures, the crystal strucrure has two forms : zinc blende (ZnS) or sphalerite (cubic), and hexagonal or wurtzite.

As such, we have seen that gallium nitride has a place of choice among such materials and enunciated the different properties, showings its particular place in the microelectronics industry. Among the two different forms, we have seen that the hexagonal structure presents many advantages over the cubic one. Also we have seen the application areas of GaN such as optical and electronic application.

We introduced after the power semiconductors market of GaN. That led to the conclusion that silicon has now reached its limits in order for it to stay competitive in those domains of applications and the necessity to switch to large band gap materials.

Lastly, we have talked about the III-nitride alloys and the AlGaN/GaN heterostructure. This showed the particularly interesting 2DEG generation for the elaboration of HEMT devices.

Chapter II

AlGaN/GaN High Electron Mobility Transistors (HEMTs)

Chapter II: AlGaN/GaN High Electron Mobility Transistors (HEMTs)

II.1 Introduction

AlGaN/GaN high-electron-mobility transistors (HEMTs) have become one of the most popular devices for high-frequency and high-power applications in recent years. Compared to traditional silicon devices, GaN material has several remarkable properties, such as better electron mobility at high electric field, wider energy bandgap (3.4 eV), higher breakdown electric field and higher saturation electron drift velocity. Such excellent material properties have made AlGaN/GaN devices the streamline technology for high-frequency and high-power applications for next-generation wireless communication systems at millimeter-wave frequencies [1].

GaN-based HEMTs are already commercially available for up to 650 V applications. However, they are currently restricted to below 1 kV mainly because of the total buffer thickness limitation with low bow and high crystal quality on large wafer diameters. SiC is another attractive wide bandgap for higher voltage but still has limited impact for the moment because of cost issues. In order to address the dynamic medium and high voltage markets beyond 1200 V while benefiting from low on-resistances, low leakage current, and low switching losses in a cost-effective way, a novel breakthrough in power electronics performance requires a new generation of materials. In this frame, the so-called ultra-wide-bandgap (UWBG) materials such as AlN (6.2 eV), which have energy bandgaps that are larger than SiC and GaN, are very promising in enabling the next leap forward in power electronics. An AlN-based material system has a unique advantage due to its prominent spontaneous and piezoelectric polarization effects, but also its flexibility in inserting appropriate heterojunctions, thus dramatically broadening the device's design space. Furthermore, AlN material represents the ideal back barrier for high voltage HEMT applications due to its large electrical breakdown field combined with a high thermal conductivity. In turn, the AlN buffer can potentially not only increase the electron confinement in a transistor channel, but can also help to boost the breakdown voltage (BV), owing to its wider bandgap, while benefiting from an enhanced thermal dissipation as compared to GaN-based devices [2].

This second chapter formally describes the AlGaN/GaN HEMTs structure and the growth techniques and substrates choice (Sapphire, GaN, AlN), also HEMTs operations naming DC characteristics, degradation of HEMT performance, breakdown mechanisms.

II.2 High Electron Mobility Transistors (HEMTs)

II.2.1 Background

The birth of the High Electron Mobility Transistor (HEMT) dates shortly after 1979 when Dingle et al. came up with the idea of using GaAs/$Al_xGa_{1-x}As$ heterojunctions to spatially separate free electrons from impurities, which promotes mobility in these gas-electron heterostructures. A joint invention between Thomson CSF (France) and Fujitsu (Japan) subsequently allowed the design of the first HEMT transistors in 1980. In 1985, the HEMT was presented as a single microwave component with the lowest noise characteristics. Initially, this transistor was used in a radio telescope in Nobeyama (Japan) which has a diameter of 45 meters. By cooling the component to the temperature of liquid helium, it is possible to pick up a signal from an interstellar molecule located a thousand light years from Earth. Later, the HEMT is implanted in television receivers to receive signals from geostationary satellites (36,000 km altitude). Then little by little, this component will make a place in our daily life. The HEMT constitutes a major evolution of MESFET (Metal/Semiconductor Junction Fet) and has taken precedence over the latter since the early 1990s [3].

The first GaN HEMTs on sapphire, silicon and silicon carbide substrates appeared in the mid-1990s. However; very interesting results in terms of power and frequency are only found at the end of the 90s. In 1999, S.T. Sheppard presented work on a GaN HEMT transistor (SiC substrate) with a power density of 6.9 W/mm at 10GHz. In the IRCOM laboratory, a HEMT GaN transistor on SiC substrate from the Tiger laboratory with 1.2mm gate development delivered an output power of 6.7 W (5.6 W/mm) and an associated power gain of 6.5dB at a frequency of 10GHz during large signal measurements in CW mode. Very good results are also obtained from GaN HEMTs transistors on silicon substrate with power densities of 1.9 W/mm at 10GHz going up to 12 W/mm at 2.14GHz [4].

Very recently, companies like CREE and SOITEC have started to offer GaN wafers, while continuing to produce much more mature SiC wafers. KK Chu's work reports a HEMT AlGaN/GaN transistor on a GaN substrate polarized at 50 V on the drain, having a power density of 9.4 W/mm at

10 GHz. We therefore note that all the results presented so far, and obtained with conventionally structured HEMTs, do not exceed 10W/mm for X-band applications [5].

This component is now widely used as a low noise component in terrestrial and space telecommunications systems, in radio telescopes, in satellite television receivers, in many electronic systems, from cell phones to motor vehicles.

II.2.2 $Al_xGa_{1-x}N$/GaN HEMTs structure

The structure of an HEMT (Figure 1) consists essentially of three different materials: the substrate, a wide bandgap material, and a lower bandgap material. The junction of these last two materials causes the formation of the two-dimensional gas of electrons at the interface, the density of which is modulated by the voltage applied to the gate of the component. The other phenomenon characteristic of the operation of a HEMT, besides the existence of an electron gas, is the Schottky junction created by the gate metal and semiconductor junction of the substrate [6].

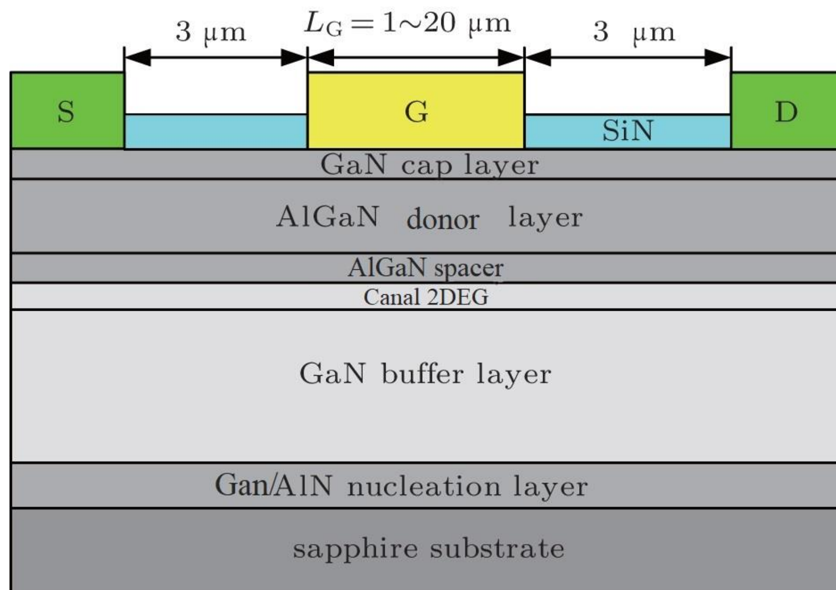

Figure II. 1 Structure of an AlGaN/GaN HEMT transistor.

The substrate: This is the layer on which the materials are grown by epitaxy. In our case, bulk GaN is not currently available at low cost and in large size, gallium nitride substrates are still very little used; we then use substrates other than GaN. The wrong choice of substrate can cause dislocations during growth which can render the component non-functional. The materials often used are silicon, sapphire and silicon carbide [6].

The nucleation layer: It is a thin layer of GaN which serves to minimize the mesh mismatch between the buffer layer and the substrate and the rate of structural defects (dislocations in particular) and to ensure to have a good crystallographic quality in order to grow the GaN crystal layer [6].

GaN buffer layer: This layer consists of the material with the smallest forbidden bandwidth, in our case it is gallium nitride (3.4eV), it is in the upper part of this layer that the two-dimensional gas is formed. It improves the confinement of electrons in the channel by reducing the injection of carriers into the substrate.

The canal (2DEG): The canal is located in the layer of unintentionally doped small gap material. This is the most important part of the HEMT: it is where the two-dimensional gas of electrons (2DEG) is created. It is the layer that determines the performance of the component through the electron transport properties in the material [6].

The spacer: This layer is produced in our case by the material with the largest gap (gallium-aluminum nitride AlGaN). This unintentionally doped film is a few nanometers thick and reduces the electron-donor interactions between the electron gas and the doped (donor) layer. Indeed, the proximity of these particles would lead to an electrostatic interaction known as Coulomb Scattering.

Without this layer, the electrons in the channel would be strongly attracted to the donor atoms of the donor layer and would therefore be confined to the AlGaN / GaN interface. This interface area has crystal defects that limit the mobility of electrons. The thinner this layer is, the more the concentration of charges in the channel increases, thus presenting a high current density, and also reducing the source resistance. The thicker it is, the more the density of charge carriers decreases, thus increasing the mobility of electrons. There is therefore a compromise with respect to its thickness [6].

The donor layer: It is in this layer that the zone of charge space forms at the Schottky junction of the grid as well as around the heterojunction. It is a layer of AlGaN wide-gap material that is doped and which provides free electrons to the structure. Its doping is generally high, using silicon which plays an important role in it because it contributes to the increase in the concentration of the electrons supplied.

The cap layer: It is a thin surface layer, formed by a low bandgap material (gallium nitride), on which good ohmic drain and source contacts are made. This layer is generally heavily doped, the

fineness of its thickness makes it possible to reduce the value of the contact resistances and therefore that of the access resistors. It also helps prevent oxidation of the AlGaN layer. In order to obtain a good Schottky gate junction, a full recess of this thickness must be performed under the gate contact [6].

An additional layer with a large gap AlGaN that is not intentionally doped can be added, it makes it possible to make a good quality gate Schottky contact or rectifier. It is initially thick and subsequently hollowed out to improve the form factor (ratio of the gate length to the total thickness of the wide gap layer) and thus better control the density of the channel carriers by the gate potential. Indeed; when the doped layer under the Schottky contact is not completely depopulated of carriers, the curvature of the conduction band favors the passage of the current by tunneling effect and a channel is created there parallel to that of the undoped layer with small gap which is none other than that of a MESFET transistor. In that case, the current controlled by the gate electrode is more or less partially associated with low mobility carriers, which degrades the performance of the device. Note that this parasitic effect, which deteriorates the transconductance gm of the transistor, appears when the gate digging is insufficient with respect to the thickness and the doping of the doped layer with a large gap, or when the gate is not sufficiently polarized. in reverse. It is important to note that undoped structures are also studied presenting a higher mobility and a lower density, due to the phenomena of spontaneous and piezoelectric polarization [7].

II.3 Growth techniques and substrates choice

The growth of good quality hexagonal layers is conditioned by the choice of substrate. Indeed, the main problem encountered with Gallium Nitride epitaxy is that there is no tuned mesh substrate for these materials. Candidates that may be used for the AlGaN/GaN heterostructure are sapphire (Al_2O_3), silicon (Si) and silicon carbide (SiC).The characteristics of these substrates are listed in (Table 1) [8].

substrats	Structure cristalline	Paramètre de maille (A°)	Conductivité thermique $(W.cm^{-1}.k^{-1})$	Coefficients de dilatation thermique α	
				$\Delta a / a(x10^{-1}k^{-1})$	$\Delta c / c(x10^{-1}k^{-1})$
Al_2O_3	Hexagonale	a= 4.758 c=12.99	0.5	7.5	8.5
4H-SiC	Wurtzite	a=3.08 c=15.12	3.3	4.2	4.68
Si (111)	Cubique	a= 5.4301	1.5	3.59	

Table II. 1 Crystallographic characteristics of the substrates used for the growth.

The mesh mismatch between the substrate and the epitaxy layer generates a stress in the layer. From a critical thickness, the layer relaxes, creating dislocations that are harmful to the quality of the material. In order to solve this problem, a nucleation layer or buffer is deposited there, to achieve homoepitaxy of the layers without stress. Despite the use of such a process, there still remains a residual stress. Its origin comes from the difference in the thermal expansion coefficients between the layer and the substrate [8].

semi-conducteurs	*Structure cristalline*	*Gap (eV) à 300K*	*Nature du gap*
Si	Cubique	1.12	Indirect
SiC	Hexagonale	2.86	Indirect
AlN	Wurtzite	6.28	Direct
GaN	Wurtzite	3.39	Direct

Table II. 2 Characteristics of semiconductors.

Ideally, the substrate is made of the same material as the transistor in order to avoid any degradation in the performance of the transistor. Among these degradations, the damage caused by crystallographic discontinuities between the material and the lower layer which constitutes its substrate.

In our case, a Gallium Nitride substrate well reduces the complexity between the two materials, thus maintaining uniformity by eliminating any mesh mismatch between the two

structures. However, such a substrate today is difficult to manufacture, because of its very high cost, and also because of the very high temperatures and pressure levels it requires to melt it. We are therefore forced to use another substrate made of a material other than GaN, so that the GaN crystal layer can grow. The only problem is that most of the substrates used for Gallium Nitride epitaxy disagree sharply with the latter [9].

Most of the transistors produced today are deposited on silicon, SiC or sapphire substrates. These two materials offer advantages thanks to their low manufacturing cost, and also to their high thermal stability. However, their main drawback is the crystal defects generated by the differences in lattice parameters with GaN. Other alternatives are proposed to reduce the complexity of this problem, by using the SOI "Silicon On Insulator" substrate for example, but the three main substrates generally used are listed below [9].

II.3.1 Silicon Carbide Substrates (SiC)

The advantages of SiC substrates are multiple. They have a low mesh mismatch with GaN of 3.5%, compared to sapphire or silicon, and very good thermal conductivity, it is the most attractive substrate. The 4H-SiC and 6H-SiC substrates are the most widely used, and have the advantage of also existing in wurtzite form, which facilitates the growth of GaN on them [10].

Polarity control is one of the key advantages of SiC over sapphire. The electrical polarity of the GaN/SiC interface strongly influences the surface morphology and crystal quality of epitaxial GaN films. Calculations of the electronic structure of the GaN/SiC [0 0 0 1] interface indicate that the strongest bonds are the Si/N and C/Ga bonds. A GaN film deposited on a face-Si SiC substrate will therefore be of the face-Ga type [0001]. The disadvantages of SiC substrates are on the one hand the very high cost, and on the other hand the surface roughness, which is on average 1 nm, compared to 0.1 nm for sapphire. This results in the need to perform surface treatments so as to polish the substrate. One method is to cause SiC to oxidize to form SiO_2, which is then etched away. Companies like Sterling Semi-Conductor produce 3 inch substrates, Nippon Steel achieves 4 inch [10].

The epitaxial GaN layers on this type of substrate thus demonstrate excellent crystallographic quality: the rate of dislocations generally remaining below 3.10^{8} cm^{-2}, in particular thanks to the addition of a nucleation layer or buffer layer in AlN, whose physical parameters allow a smoother transition between the SiC crystal lattice and that of GaN. This transition is further improved by the

addition of nucleation superlattices, a technique consisting in integrating between the substrate and GaN, a succession of AlN/GaN layers. It is thus, of all the substrates, the one which foreshadows at the head when microwave power applications are envisaged. Unfortunately, it remains extremely expensive. For the 6H type, the mesh mismatch with GaN is 3.5%. It is an electrically conductive material that can be n or p doped and its thermal conductivity is significantly higher than that of sapphire [11].

II.3.2 Sapphire Substrates *(Al_2O_3)*

Sapphire is the most used for the manufacture of light emitting diodes and laser diodes. However, it has several major flaws. In fact, the mesh mismatch with GaN is 16% (after rotation of the epitaxial layer relative to the substrate). This mismatch induces dislocation densities of the order of 1010 cm^{-2}. However, with adequate nitriding and an optimized buffer layer deposited at low temperature, for example of AlN, very good quality GaN films with a dislocation density of less than 2×10^9 cm^{-2}can be obtained. On a sapphire substrate, growth by MOVPE makes it possible to obtain GaN of the Ga-face type, while that by MBE makes it possible to obtain GaN face-Ga or N-face. The disadvantages of sapphire are low thermal conductivity and great difficulty in being cut. One of the cutting methods consists in making a groove with a laser, then in engraving in this groove with a diamond saw, to finish by a cleavage. Moreover, the substrate is in this case removed by "lift off" and replaced by a substrate of higher thermal conductivity. Finally; sapphire is an insulator, which does not allow direct electrical contact to be placed on the substrate [12].

II.3.3 Silicon Substrates (Si)

The silicon substrate is very attractive not only because it has good surface morphology and is available at low cost, but also because it allows integration of GaN-based devices into silicon microelectronics. Nevertheless, GaN shows a lattice mismatch with Si (111) of about 17% associated with a thermal expansion coefficient mismatch greater than 35%.

Unlike substrates (Al_2O_3) and SiC, silicon Si has a larger mesh than that of GaN. As a result, GaN is by definition in extension when it is epitaxied on Si (111) causing the formation of dislocations and cracks. A more complex nucleation layer composed of several sublayers of AlN and GaN (superlattice) is then produced, the growth conditions of which are different from those used for the previous substrates. The growth of the GaN layer (buffer) is then carried out on this super network [13].

II.4 HEMTs operation

In the most common HEMT structures, the wide bandgap barrier is doped n-type while the narrow bandgap channel remains undoped. As a result, electrons diffuse from the wide bandgap material into the narrow bandgap material to minimise their energy. This process continues until a balanced Fermi level is formed in the two materials and equilibrium is established. Because of the resulting electrostatics, a new triangular well forms on the narrow bandgap side of the heterojunction. Which we call it as two dimensional quantum well and the electrons confined inside the well is called Two Dimensional Electron Gas (2DEG). The n-doped barrier in the device supplies electrons to the undoped channel, thus spatially separating the channel charge carriers from their ionised donors. In this manner, the heterostructure channel is capable of delivering high carrier concentration with high mobility as impurity scattering is minimised in the undoped channel. As an added advantage, surface scattering is also reduced by moving the current-carrying region below the barrier to understand the principle of operation and techniques [14].

II.4.1 DC characteristics

HEMT, although different to a conventional MOSFET in terms of operation, is still a field effect transistor. Thus as a transistor it was developed in order to control large currents using small driving signals. HEMTs have a high potential especially in the high power and high frequency applications. To characterize the DC properties of a transistor a series of graphs is used, among which the I-V (current-voltage) characteristics called output and transfer characteristics are most known.

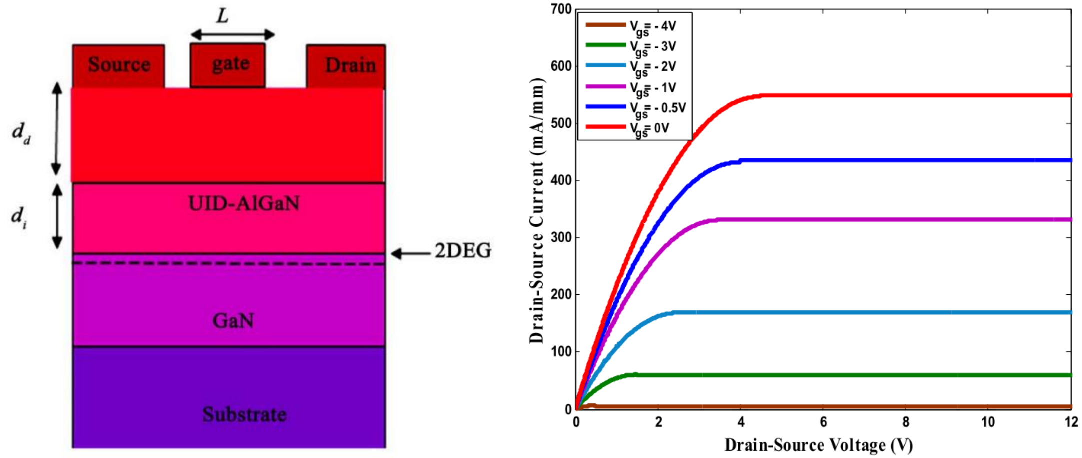

Figure II. 2 Structure for HEMT simulation (left) and theoretical ideal characteristics Ids-Vds for an AlGaN/GaN HEMT t different gate Voltage (right).

HEMT primarily works in depletion mode, i.e. current flows through the device even with no gate drive voltage. Voltage which has to be applied on the gate electrode in order to stop the current flow is called the pitch off voltage Vp. The best way to understand the HEMT electrical behavior is to develop a theorethical model and simulate the I-V characteristics.

Figure 2 (left) shows the cross-sectional view of an AlGaN/GaN HEMT used for the simulation. The layer sequence is, from top to bottom, metal/n-AlGaN/undoped-AlGaN/undoped-GaN with a 2-DEG formed at the unintentionally doped (UID)-AlGaN/GaN interface.

Figure 2 (right) shows the output Current-Voltage characteristics for different gate voltage Vgs ranging from -4 V to 0 V where -4 V is pitch off voltage Vp. For better understanding of these characteristics it is good to know the HEMT operation principle described in chapter 3.3. These characteristics correspond to an ideal HEMT structure, i.e. without considering the anomalies that may be present in this type of component. It appears clearly that the saturated drain current increases when increasing gate voltage [14].

Common Source Transistor Characteristics

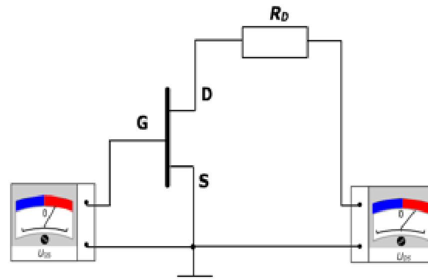

Transfer characteristics

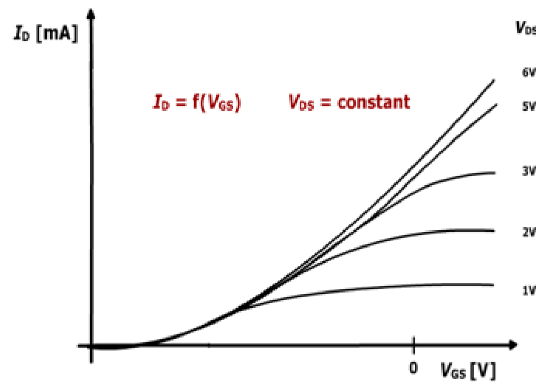

Figure II. 3 HEMT DC characteristics.

A transfer characteristic shown on (Figure 3) displays the relation between gate voltage and drain current with a constant drain-source voltage V_{ds}.

II.4.2 Degradation of HEMT performance

High-field degradation characteristics refer to the possible degradation effect of AlGaN/GaN HEMT devices after the application of the enhanced electric field. At present, the primary explanation for the degradation of AlGaN/GaN HEMT devices under strong electric field stress is the thermionic electron effect. The thermionic electron will lead to the capture and generation of surface state traps between the gate and drain, thus affecting the performance of devices and causing device degradation. Some studies believe that the inherent traps will capture the thermal electrons, while others believe that the thermal electrons themselves will form new defects. Actually, the thermionic electron effect could not be used to explain all of the high-field degradation phenomena. The device lacks channel thermal electrons under the off-state stress of the large electric field. The experimental results show that the device will also degrade under off-state stress. It is suggested that there may be other mechanisms for degradation of the device under off-state stress [14].

II.4.2.1 Off-State Stress

A characteristic curve comparing reference, off-state stress condition, and recovery condition is shown in Figure 4. It can be seen from the transfer characteristic curve of Figure 4.a that, after stress, the maximum transconductance and drain of the device current decreased. Among them, the threshold voltage was unchanged, the maximum transconductance G_{max} was reduced by 24.9%, and the maximum drain current was reduced by 31%. Nevertheless, the transfer characteristic curve of the device was restored to the pre-stress level after the device was static for 72 h. This phenomenon is generally attributed to the fact that, after stress, the electrons of the device—under the action of astrong electric field—obtain enough energy and enter the AlGaN barrier layer or the device surface to be captured by traps. Thus, the concentration of 2DEG in the channel decreased, which was macroscopically shown as the decrease of output leakage current of the device. The degradation of the characteristic curve was due to the inherent trapped carriers in the device. After storing the sample for a while to recover, the trap released the trapped carrier and the device characteristics were restored to the pre-stress level [15].

(Figure 4.b) shows the variation of the gate leakage current curve of the device. It can be seen that, after stress, the gate leakage current increased by nearly two orders of magnitude. This may be because the electric field direction generated by the negative gate voltage acting on the AlGaN barrier layer is the same as that of the AlGaN polarization electric field, and the two electric fields interact with each other. As a result, the barrier layer of AlGaN was subjected to a more significant tensile stress, which stretched the lattice structure and produced new defects in the material. The new trap-assisted carrier tunneling passed through the AlGaN barrier layer and formed a new gate current leakage channel—that is, the gate leakage current of AlGaN/GaN HEMT devices increased after stress. Moreover, the gate leakage current was unrecovered, which was consistent with the post-stress curve. It is further indicated that new traps introduced under off-state stress caused the gate leakage channel and these new defects could not be recovered with the removal of stress [16].

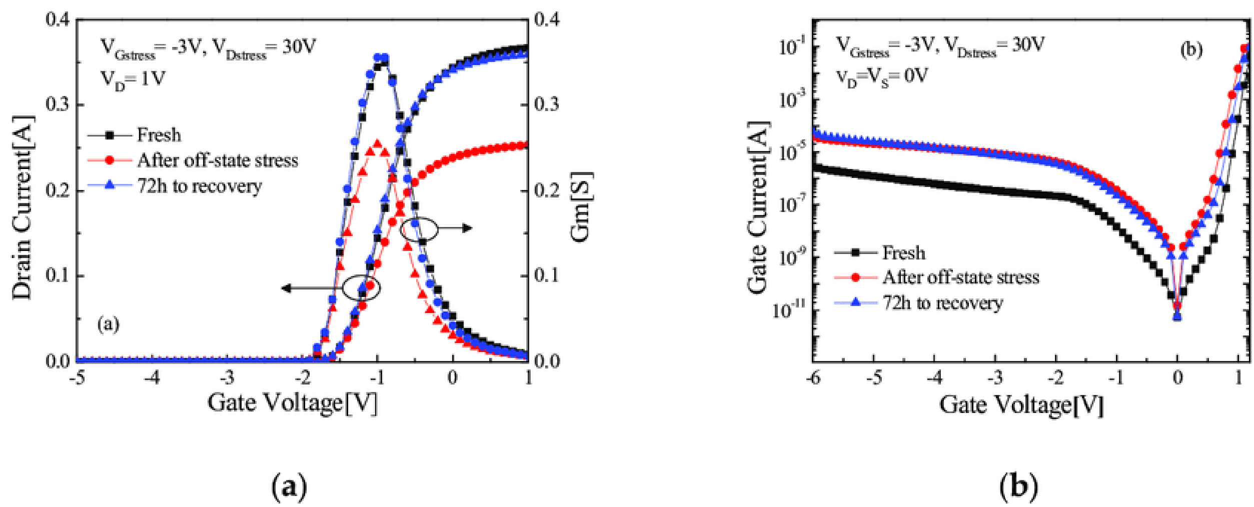

Figure II. 4 Different conditions of typical DC characteristic curves. (a) Transfer characteristic and transconductanceharacteristics; (b) gate leakage current.

II.4.2.2High-Temperature Stress

Figure 5 shows a representative curve of the DC characteristics of AlGaN/GaN HEMT devices at different ambient temperatures. It can be seen intuitively from Figure 5.a that, as the ambient temperature increased the transconductance peak and drain current of the device continuously decreased. The threshold voltage had slightly negatively drifted but the change was not obvious. The main reason was the decrease of the carrier saturation velocity in the high-temperature environment [17].

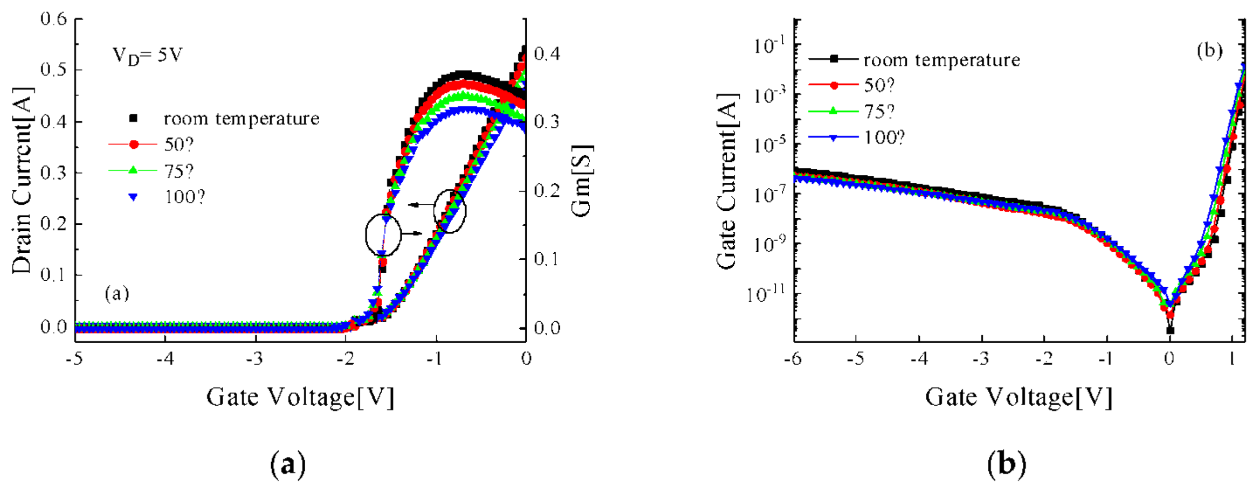

Figure II. 5 Different conditions of typical DC characteristic curves. (a) Transfer characteristic and transconductanceharacteristics; (b) gate leakage current.

II.4.3 Breakdown mechanisms

Thanks to the recent advancements in the growth and fabrication processes, the performance of high electron mobility transistors (HEMTs) based on GaN has significantly improved. The main advantages of using GaN as a material for the realization of HEMTs are:

- The high sheet charge density (>10^{13} cm^{-2}) of the two dimensional electron gas (2DEG), which results in a low on-resistance of the transistors.
- The high thermal conductivity of GaN (>2 W cm^{-1} K^{-1}), which permits to reach high levels of power dissipation while keeping the channel temperature low.
- The high breakdown field (3.3 MV/cm), which allows to fabricate devices with breakdown voltages in the order of hundreds or thousands of volts, depending on gate drain spacing and on buffer thickness. These unique features make GaN an almost perfect material for the manufacturing of high power transistors: thanks to the recent efforts of the scientific and industrial communities, GaN-based transistors with breakdown voltages in excess of 1.5–1.9 kV have been recently demonstrated, thus clearing the way for the adoption of HEMTs in power electronics. Moreover, thanks to the low (on-resistance) *(device capacitance) product, GaN-based power HEMTs can reach high switching frequencies (>40 MHz), and can therefore be used for the fabrication of high efficiency power conversion systems: converters with efficiencies in excess of 96–98% have already been demonstrated, thus proving the superiority of GaN with respect to more conventional semiconductors for power electronics.

Despite the high performance of GaN-based HEMTs, the lifetime of these devices can be shorter than expected, due to the existence of a number of physical mechanisms responsible for device degradation. Recent studies demonstrated that GaN HEMTs may degrade due to the following processes:

- Degradation of the gate Schottky junction induced by off-state stress This mechanism induces an increase in the gate leakage current, due to the generation of localized shunt paths in proximity of the gate edge
- Semi-permanent or permanent degradation due to hot electrons: This mechanism occurs when the devices are operated in the on-state, and in most of the cases results in a decrease in drain current, due to the accumulation of negative charge close to the gate edge and/or in the gate–drain access region.)

- Delamination of the passivation, due to the exposure to high temperature/power levels, which may result in additional charge trapping and leakage processes.
- Time-dependent degradation processes, due to the generation of defects within the AlGaN/GaN heterostructure. Besides these mechanisms, power devices operated at high drain voltages may show important breakdown (BD) processes breakdown consists in a rapid increase in drain current, which occurs in the off-state when the drain voltage reaches a critical value. Breakdown may be catastrophic (i.e., induce a sudden failure of the devices); this typically happens when BD measurements are carried out in voltage controlled mode, by increasing the drain voltage until a un-controllable increase in drain current is triggered. A sustainable breakdown condition can be reached if the measurements are carried out in current-controlled mode: by using this method it is possible to separately evaluate the contribution of gate, source, and bulk leakage to the overall BD current, thus extracting information on the physical origin of breakdown for several operating conditions [17].

As can be understood, breakdown represents an important problem for high power/high voltage HEMTs: for this reason, over the past years several groups have investigated the physical origin of BD, with the aim of developing models to explain this phenomenon, and of proposing technological improvements to increase the robustness of the devices. This study reviews the physical mechanisms responsible for breakdown in GaN-based power transistors: to this aim, original results are compared with data taken from the literature. The following, relevant, breakdown mechanisms are discussed in detail:

- Source–drain breakdown, due to short-channel effects, and/or punch-through.
- The presence of relatively high breakdown current components at the gate, which can be either related to the leakage through the Schottky junction, or to surface related conduction.
- Vertical breakdown, which can be due to a poor compensation of the buffer, to the use of a conductive substrate, and can be limited by the adoption of suitable back barrier or heterostructure configurations.
- Impact ionization mechanisms, that may induce a significant increase in drain current due to the generation of electron–hole pairs close to the gate [17].

II.5 Summary

Throughout this second chapter, we have introduced the High Electron Mobility Transistors (HEMTs), its background and the birth of it and how scientists manage to create it, we talked about the operating principle of AlGaN/GaN HEMTs, its structure and the different layers that compose it.

Afterwards, we have presented the growth techniques and the different substrates choice such as Silicon Carbide Substrates (SiC), Sapphire Substrates (Al_2O_3) and Silicon Substrates (Si); we have talked briefly about their advantages and disadvantages.

In the last part, we have talked about HEMTs operation naming their dc characteristics, the degradation of HEMT performance and the breakdown mechanisms. The HEMTs materials remain prime candidates for high power applications.

Chapter III

Simulation results and discussion

Chapter III: Simulation results and discussion

III.1 Introduction

In recent years, and because of the high costs of experimentation, researchers have turned to simulation. Simulation is therefore widely used in the electronic field and indeed makes it possible to determine the most important parameters for the operation of devices, to minimize losses and to optimize the physical and geometric parameters of these devices.

Despite the interesting performance of the HEMT transistor, the operation of this transistor in particular for power applications generates self-heating due to the Joule effect. This effect is responsible for the degradation of the transport properties of materials and therefore for the degradation of the performance of this transistor. These thermal effects can also lead to the destruction of this component. It is therefore necessary to take into account the heat dissipation and its influence on all the parameters of the component, and thanks to their very high breakdown voltages and their high sheet carrier densities, AlGaN/GaN HEMTs are a very promising solution for high-power and high-frequency applications. The progress made on their technology over the last few years now make them usable in systems, and hence, there is a need for electrical models. Many topologies and solutions to extract models are reported in the literature [1].

The objective of this chapter is to simulate and study the modeling of an AlGaN/GaN HEMT using the MATLAB software, so we propose a model definition and study it to make a HEMT device structure, and the results are evaluated for a variety of IV characteristics.

III.2 About Matlab

The name MATLAB stands for MATrixLABoratory. MATLAB was written originally to provide easy access to matrix software developed by the LINPACK (linear system package) and EISPACK (Eigen system package) projects, it is a programming package specifically designed for quick and easy scientific calculations and I/O. It has literally hundreds of built-in functions for a wide variety of computations and many toolboxes designed for specific research disciplines, including statistics, optimization, solution of partial differential equations, data analysis [2].

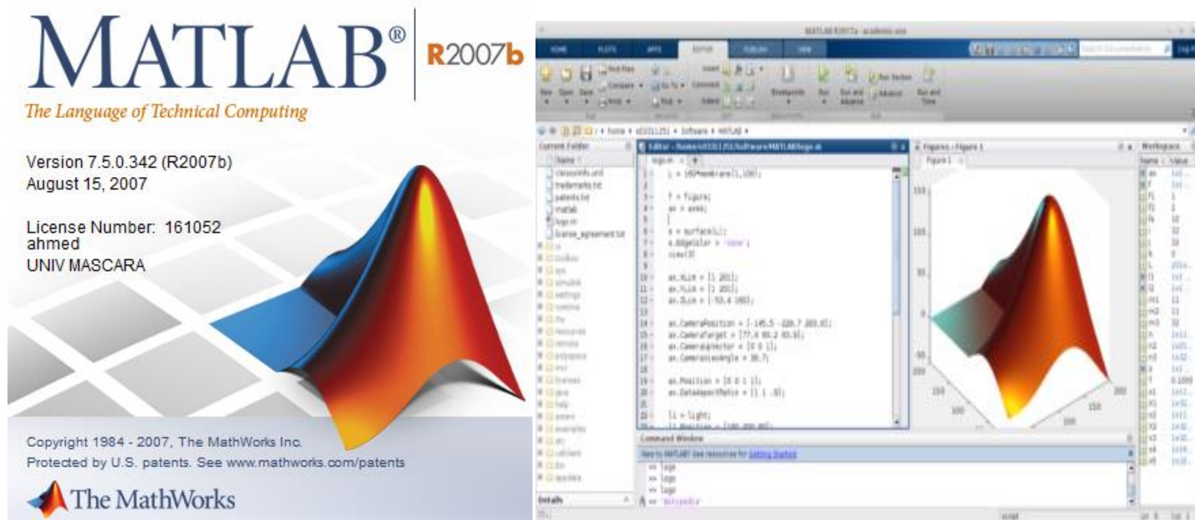

Figure III. 1 Matlab logo (left), creation of Matlab logo (right).

MATLAB is a high-performance language for technical computing. It integrates computation, visualization, and programming environment. Furthermore, it is a modern programming language environment: it has sophisticated data structures, contains built-in editing and debugging tools, and supports object-oriented programming. These factors make MATLAB an excellent tool for teaching and research [3].

MATLAB has many advantages compared to conventional computer languages (e.g., C, FORTRAN) for solving technical problems. MATLAB is an interactive system whose basic data element is an array that does not require dimensioning. The software package has been commercially available since 1984 and is now considered as a standard tool at most universities and industries worldwide [4].

It has powerful built-in routines that enable a very wide variety of computations. It also has easy to use graphics commands that make the visualization of results immediately available. Specific applications are collected in packages referred to as toolbox. There are toolboxes for signal processing, symbolic computation, control theory, simulation, optimization, and several other fields of applied science and engineering [4].

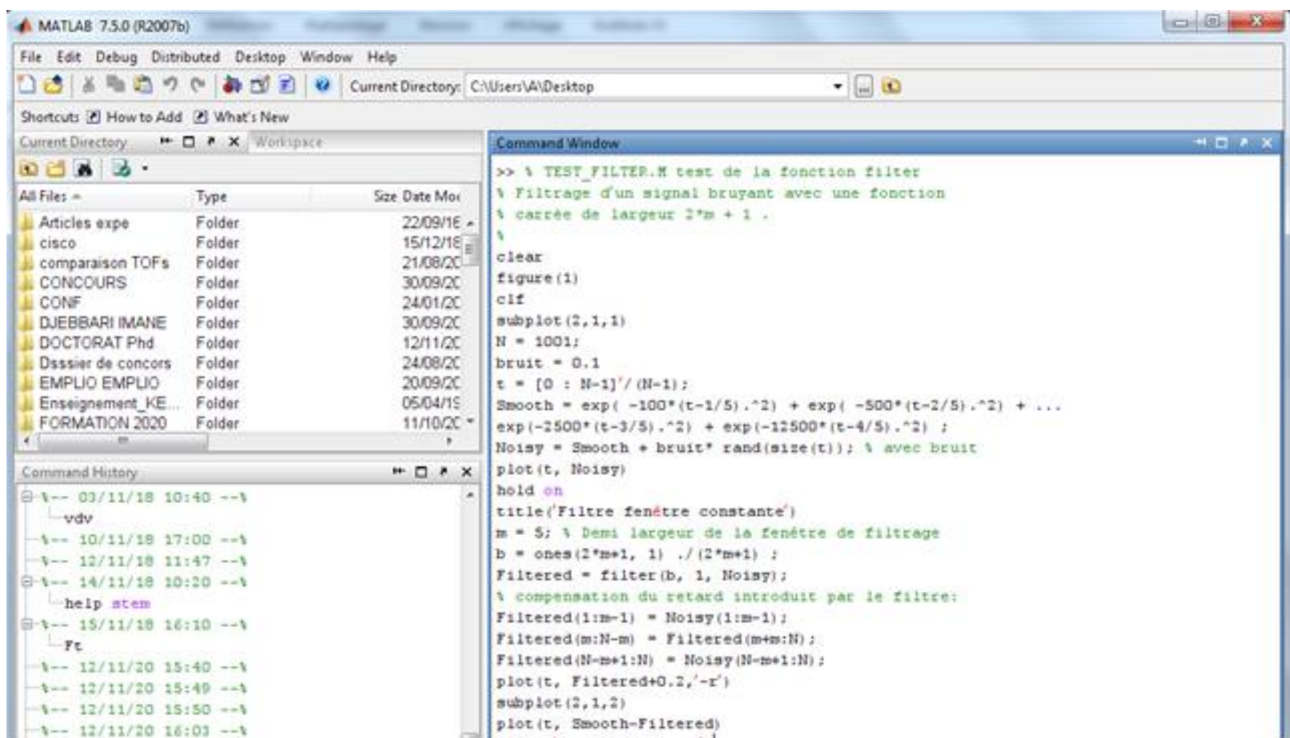

Figure III. 2 Matlab example program.

III.3 Model definition

symbol	*Description*
q	The electron charge
V_{th}	Thermal Voltage
ε	The dielectric permittivity of AlGaN
d	Thickness of AlGaN layer
E_f	Position of the Fermi level
E_0	Position of the first enery level in the quantum well
E_1	Position of the second enery level in the quantum well
D	Density of states
γ_0, γ_1	Parameters determined from experiment
n_s	Density of electron in the 2DEG
C_g	Gate Capacitance per unit area (ε/d)

Table III. 1 List of Symbols.

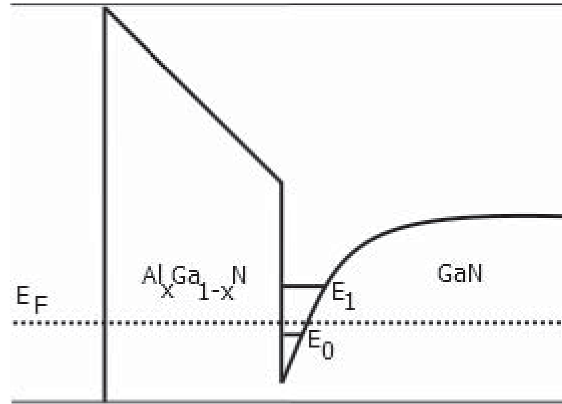

Figure III. 3 Heterostructure interface and energy band profile of an AlGaN/GaN HEMT.

ANALYTICAL CURRENT MODEL

A. Core Current Model

In heterostructures such as AlGaN/GaN and AlGaAs/GaAs the charge density per unit area accumulated in the potential well at the interface can be calculated with the assumption of a quasi-constant electric field in the potential well (triangular well approximation) and two subbands as [5]

$$n_s = DV_{th}\left[\ln\left(e^{(E_f - E_0)/V_{th}} + 1\right) + \ln\left(e^{(E_f - E_1)/V_{th}} + 1\right)\right] \tag{1}$$

These subbands are given by [6]

$$E_0 = \gamma_0 n_s^{2/3} \text{ and } E_1 = \gamma_1 n_s^{2/3} \tag{2}$$

Where γ_0 and γ_1 are constants estimated from Shubnikov De Hass or cyclotron resonance experiments [5] (all other symbols have standared definition as given in Table 1). When the gate depletion and channel depletion overlap to give a fully depleted barrier layer, the carrier density is given by [7]

$$n_s = \frac{\varepsilon}{qd}(V_{g0} - E_f) \tag{3}$$

where$V_{g0} = V_g - V_{OFF}$, where V_{OFF} is the cutoff voltage.

In the triangular quantum well created at the interface of AlGaN/GaN, the second energy level is much higher than the first one and is well above the Fermi level for the whole operating

range of the gate voltage [8] (see Figure 1). Thus, here the contribution of only the first energy level is considered. Therefore, (1) can be approximated as

$$n_s = DV_{th} \ln\left(\exp\left(\frac{E_f - E_0}{V_{th}}\right) + 1\right) \tag{4}$$

The expressions of E_0 and E_f from (2) and (3), respectively, can be used in (4) to establish a correlation between V_{g0} and n_s given as

$$V_{g0} = \frac{qdn_s}{\varepsilon} + \gamma_0 n_s^{2/3} + V_{th} \ln\left(\exp\left(\frac{n_s}{DV_{th}}\right) - 1\right) \tag{5}$$

The exponential term in (5) can be expanded into a Taylor series and the first few terms can be used. The first term gives a good approximation. In addition, (5) can be extended to any channel point by considering V as the local quasi-Fermi potential. Therefore, we have

$$V_{g0} - V = \frac{qdn_s}{\varepsilon} + \gamma_0 n_s^{2/3} + V_{th} \ln\left(\frac{n_s}{DV_{th}}\right) \tag{6}$$

An analytical current model can be formulated using the definition of the drain current along the channel given as

$$I_{ds} = W\mu q n_s \frac{dV}{dx}, \quad \text{or} \qquad I_{ds} = \frac{W}{L}\int_{V_s}^{V_d} q n_s \mu dV \tag{7}$$

Where W is the width, L is the channel length, μ is the low field mobility of the device, and V_d and V_s are the drain and source voltages, respectively. dV with respect to the charge density obtained from the derivative of (6), which enables integration over the charge density, can be given as

$$dV = -\left(\frac{qd}{\varepsilon} + \frac{2}{3}\gamma_0 n_s^{-1/3} + V_{th} n_s^{-1}\right) dn_s \tag{8}$$

Using (8) in (7) and integrating from source to drain will give a simple analytical model of the drain current, which can be written as

$$I_{ds} = -\frac{q\mu W}{L}\left[\frac{qd}{2\varepsilon}(n_D^2 - n_S^2) + \frac{2}{5}\gamma_0\left(n_D^{5/3} - n_S^{5/3}\right) + V_{th}(n_D - n_S)\right] \tag{9}$$

Where n_S and n_D are the charge carrier concentrations at the source and drain, respectively, and d is the barrier layer thickness and all the other symbols have the standard definition. The current model in (9) can satisfactorily be used to reproduce the I–V characteristics of a long channel device.

n_S and n_D can be obtained iteratively from (6). Anyway, sufficiently accurate explicit expressions would make the model computationally faster.

Here, we have used an approximate unified explicit expression that covers all the operating regions from deep subthreshold to full active gate bias to obtain the charge carrier concentrations at the source and drain [9]. Therefore, n_S is calculated as

$$n_s = \frac{2V_{th}(C_g/q)\ln(1+\exp(V_{g0}/2V_{th}))}{1/H(V_{g0})+(C_g/qD)\exp(-V_{g0}/2V_{th})} \quad (10)$$

Where C_g is the gate capacitance. The function $H(V_{g0})$ in the denominator, which simulates the nonlinear behavior in the above threshold region, is given as

$$H(V_{g0}) = \frac{V_{g0}+V_{th}[1-\ln(\beta V_{g0n})]-\frac{\gamma_0}{3}\left(\frac{C_g V_{g0}}{q}\right)^{2/3}}{V_{g0}\left(1+\frac{V_{th}}{V_{g0d}}\right)+\frac{2\gamma_0}{3}\left(\frac{C_g V_{g0}}{q}\right)^{2/3}} \quad (11)$$

Where $\beta = C_g/qDV_{th}$, and the two interpolation functions V_{g0n} and V_{g0d} of V_{g0} are given by

$$V_{g0n} = \frac{V_{g0}\alpha_n}{\sqrt{V_{g0}^2+\alpha_n^2}} V_{g0d} = \frac{V_{g0}\alpha_d}{\sqrt{V_{g0}^2+\alpha_d^2}} \quad (12)$$

Where $\alpha_n = e/\beta$ and $\alpha_d = 1/\beta$.

The calculation of n_D is indicated in the next section.

B. Saturation Voltage

The saturation voltage is modeled using the approach given by

$$V_{sat} = \frac{v_{sat}V_{g0}}{v_{sat}+(\mu_{eff}/2L)V_{g0}} \quad (13)$$

Where μ_{eff} is the effective mobility and v_{sat} is the saturation velocity. Equation (13), which is commonly used in many MOSFET models has been adopted for the case of HEMTs here [10], [11]. Replacing the first factor V_{g0}on the left with$Q_s/2C_g$, where Q_s is the charge per unit length at the source, the relation will also be valid in the weak inversion as the latter term tends to V_{g0}in strong inversion and to zero in weak inversion. Therefore, (13) can be written as

$$V_{sat} = \frac{Q_s}{2C_g} \frac{v_{sat}}{v_{sat}+(\mu_{eff}/2L)V_{g0}} \tag{14}$$

According to (14), V_{sat} will tend to zero in weak inversion while its theoretical value in this region is $2V_{th}$. This can be avoided using an effective source end charge sheet density, which tends to Q_s in strong inversion and leads to the correct value of V_{sat} in the weak inversion region. This is given by

$$Q_{seff} = Q_s + 4V_{th}C_g \frac{v_{sat}}{v_{sat}-\frac{\mu_{eff}}{L}V_{th}}. \tag{15}$$

Once the saturation voltage is calculated, we obtain the effective drain voltage, which is designed to give a smooth transition between the applied drain-source voltage, V_{ds}, for $V_{ds} < V_{sat}$ and approaches V_{sat} for$V_{ds} \geq V_{sat}$

$$V_{d,eff} = V_{sat}\left[1 - \frac{\ln\left[1+\exp\left(1-k\frac{V_{ds}}{V_{sat}}\right)\right]}{\ln[1+e]}\right] \tag{16}$$

Where k is the transition width parameter.

The charge carrier concentration at the drain, n_D, is calculated using (10) by replacing $V_{g0}$with$V_{gdo} = V_{g0} - V_{d,eff}$.

C. Channel Length Modulation and Short Channel Effects

The CLM, which occurs for drain voltages higher than the saturation voltage, is a decrease in the effective length of the channel as the saturation point starts to move toward the source. The effect of CLM on the drain current is modeled as follows [12]:

$$I_{ds,CLM} = I_{ds}(1 + \lambda V_d) \tag{17}$$

Where λ is a CLM parameter, I_{ds} is the core current model, and $I_{ds,CLM}$ represents the current model after the CLM correction.

The SCE is introduced as a shift in the cutoff voltage given by [13]

$$V_{OFF,SCE} = V_{OFF} - V_d/SCE \tag{18}$$

Where $V_{OFF,SCE}$ is the cutoff voltage when SCE occurs and SCE is the SCE parameter determined from measurement data.

D. Self-Heating Effect

Self-heating is well known to affect the device performance in high power conditions. Since AlGaN/GaN devices are becoming the main candidates of many high power applications, it is necessary to incorporate self-heating effects (SHEs) in the models of these devices. To model the self-heating, it is important to consider the additional temperature incurred due to the SHE. This is simply given as [12], [14]

$$\Delta T = P_d R_{th} \tag{19}$$

Where P_d is the dissipated power, which can be given as $P_d = I - V$and R_{th} is the thermal resistance of the device. The actual working temperature of the device, T_{actual}, can then be corrected by adding (19) to the ambient temperature of the device

$$T_{actual} = T_{ambient} + \Delta T \tag{20}$$

Where $T_{ambient}$ is the ambient temperature.

CHARGE AND CAPACITANCE MODELS

A gate charge model is developed using the simple unified charge control model. Once the complete charge expression is obtained the expressions for the gate-source and gate-drain capacitances are derived.

A. Charge Model

The gate charge can be obtained by integrating the charge density along the channel over the gate area

$$Q_G = W \int_0^L q n_s(x) dx. \tag{21}$$

In (21), dxcan be substituted from (7), which will change the integration variable from x to V. Therefore, we have

$$Q_G = \frac{W^2 q^2 \mu}{I_{ds}} \int_{V_s}^{V_d} n_s^2 dV. \tag{22}$$

After substituting for I_{ds} from (7) in (22), the gate charge is given as

$$Q_G = WLq\left(\frac{\int_{V_S}^{V_d} n_s^2 dV}{\int_{V_S}^{V_d} n_s dV}\right). \tag{23}$$

The two integrals at the numerator and denominator in (23) can be represented as $f(n_s)$and $g(n_s)$, respectively, and integrating after changing the integration variable using (8) gives

$$f(n_s) = \frac{\text{qd}}{3\varepsilon}(n_D^3 - n_S^3) + \frac{1}{4}\gamma_0\left(n_D^{8/3} - n_S^{8/3}\right) + \frac{1}{2}V_{th}(n_D^2 - n_S^2) \tag{24}$$

$$g(n_s) = \frac{\text{qd}}{2\varepsilon}(n_D^2 - n_S^2) + \frac{2}{5}\gamma_0\left(n_D^{5/3} - n_S^{5/3}\right) + V_{th}(n_D - n_S) \tag{25}$$

Note that $g(n_s) = -I_{ds}L/q\mu W$.

III.4 HEMT Device Structure

(Figure 4) shows the device AlxGa1-xN/GaN nanostructures HEMTs consisting of 100 nm GaN buffer layer, where deposited on the SiC substrate. The SiC substrate is highly doped with a free electron. On top 100 nm of the GaN buffer layer, followed by the growth of a 3 nm of $Al_xGa_{1-x}N$ spacer layer and with 12 nm of $Al_xGa_{1-x}N$ barrier, It can be seen here that the barrier layer AlGaN under the gate is doped, while the GaN buffer layer is undoped. The source and drain contacts are ohmic, while the gate is a Schottky barrier of (Ni and Ti) [15]. For low values of drain-to-source bias, a current flows from drain to source through the electron channel. The carrier sheet density and consequently the conductivity of the channel are controlled by the gate bias. The gate width is a physical device dimension that is of primary importance to the determination of device behaviour. The device current is directly proportional to the gate width because the cross-section area available for the channel current is proportional to Z. For low-noise, low-current applications relatively small-gate-width devices are utilized. In contrast, large-gate-width devices are typically used for power applications [16].

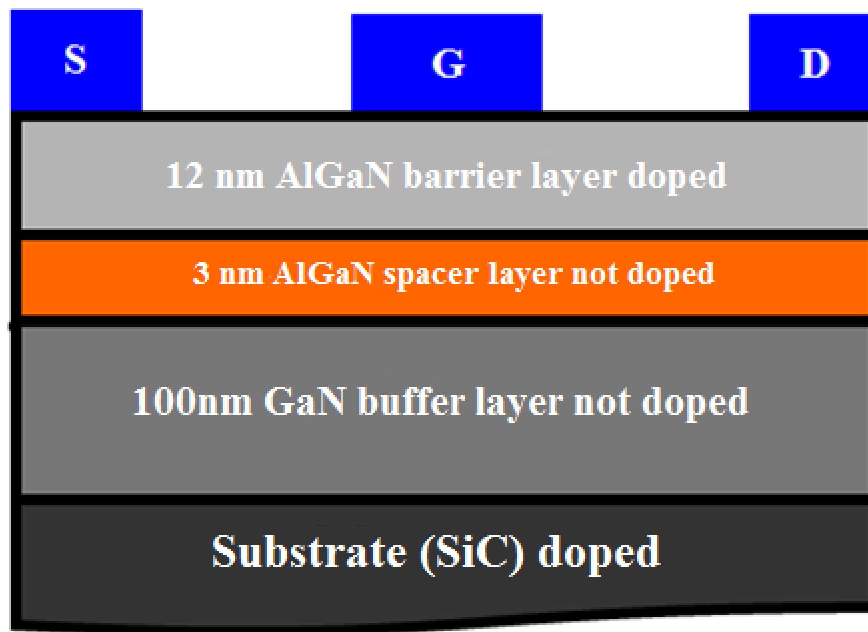

Figure III. 4 Cross sectional view of $Al_xGa_{1-x}N/GaN$ nanostructures HEMTs using for simulation.

III.5 Resultats and Discussion

III.5.1 Simulation resultats

A. Simulation at different gate voltages

(Figure 5) shows the electrical characteristics of HEMTs transistors are calculated at gate voltage V_{GS} is varied from -1 V to 1 V with a step of 0.5 V. Our simulation results indicate that increasing of the positive bias applied to the gate increases the depth of the potential well at the $Al_xGa_{1-x}N/GaN$ interface. Therefore, these results in enhanced sheet carrier density of the electron channel thus we can find that the drain current increase.

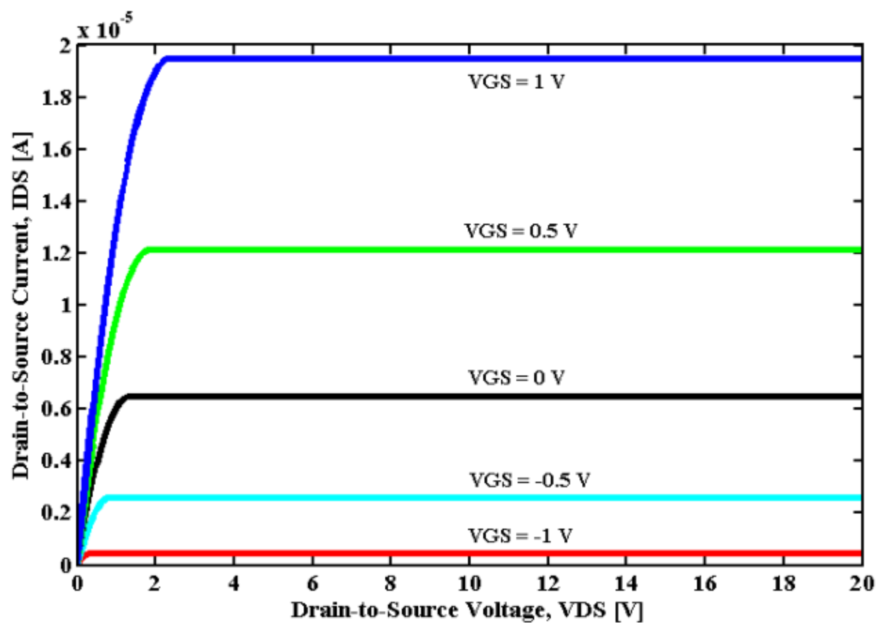

Figure III. 5 Electrical characteristics of $Al_xGa_{1-x}N$/GaN HEMTs for different gate-to-source voltage.

B. Variation in the gate width Z

The gate width Z is a physical device dimension that is of primary importance to the determination of device behaviour. For that we investigate the influence of the gate width on the current-voltage characteristics of our device. The result of our simulation is shown in (Figure 6). We have observed a high drain current saturation with the increasing of the gate width, which have great significance for high power applications.

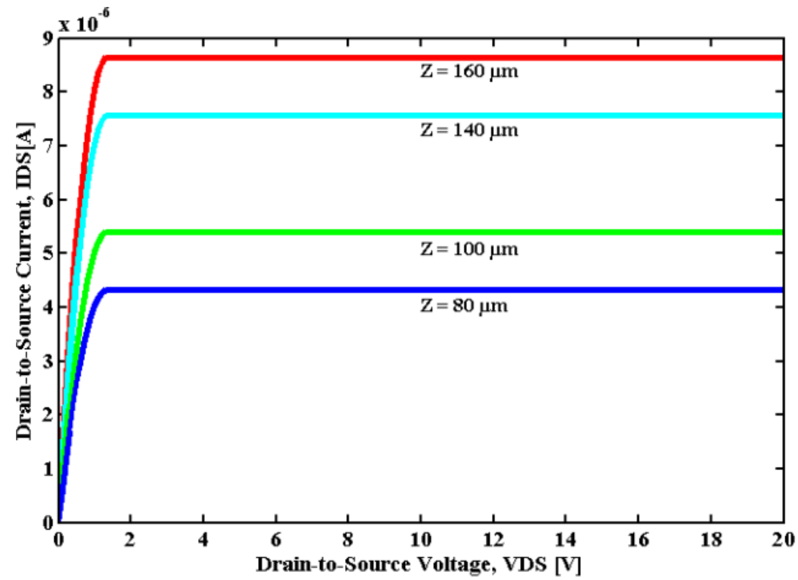

Figure III. 6 Electrical characteristics of $Al_xGa_{1-x}N$/GaN HEMTs for different gate width Z.

C. Variation of the doping layer thickness $Al_xGa_{1-x}N$

(Figure 7) shows the simulated I_{DS}–V_{DS} characteristics of the model of $Al_xGa_{1-x}N$/GaN nanostructures HEMT with different thickness of $Al_xGa_{1-x}N$ doped barrier layer varied from (10 to 17) nm are calculated at $V_{GS} = 1$ V. Our simulation results indicate that the fabrication of the $Al_xGa_{1-x}N$/GaN nanostructures HEMT by using a thinner doped barrier layer successfully increasing the current drain. This results in increases the sheet carrier concentration of the electron channel, therefore increasing current conduction, which is critical to obtain a maximum drain current.

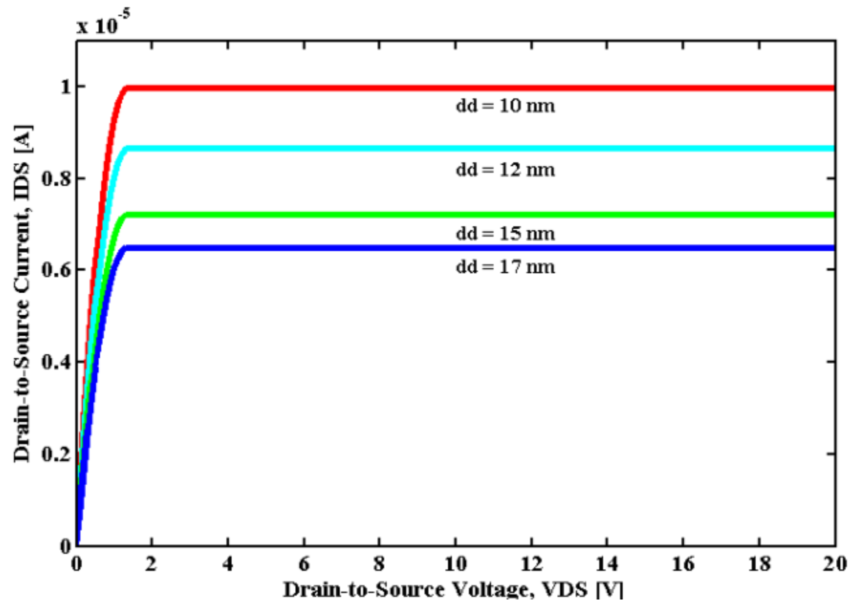

Figure III. 7 Electrical characteristics of $Al_xGa_{1-x}N$/GaN HEMTs for different Barrier layer thickness.

D. Variation of the $Al_xGa_{1-x}N$ spacer layer thickness

The $Al_xGa_{1-x}N$ spacer layer is used to separate spatially the carriers from the doped region to the channel. (Figure 8) shows the electrical characteristics of $Al_xGa_{1-x}N$/GaN nanostructures HEMT for different spacer layer thickness. We have observed that the drain current decrease when the spacer layer increase due to the decreasing of the carrier density transferring to the channel layer.

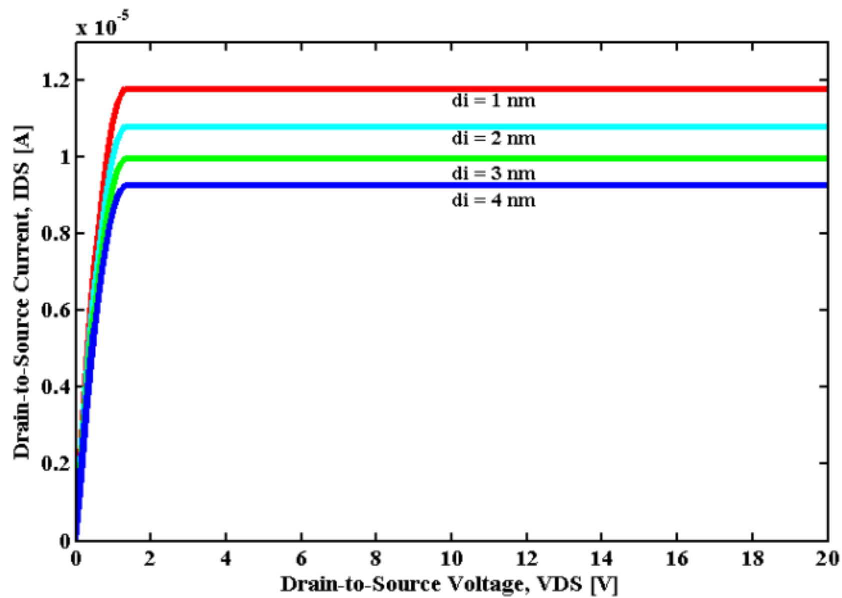

Figure III. 8 Electrical characteristics of AlxGa1-xN/GaN HEMTs for different spacer layer thickness.

III.6 Conclusion

The main focus of this work is the simulation results of the electrical characteristics of $Al_xGa_{1-x}N/GaN$ nanostructures HEMTs, by using samples with a different gate bias, Al content, different gate width, and with different thickness of $Al_xGa_{1-x}N$ barrier layer and spacer layer.

Furthermore, our simulation results indicate that, the $Al_xGa_{1-x}N/GaN$ nanostructures HEMTs provide higher ON-current at Z = 160 µm, d_d= 10 nm and d_i = 1nm V_{GS} = 1 V. Moreover, the negative enhancement observed in V_{Th} for higher doping with higher Al content is due to the fact that higher negative voltage is required to deplete a higher density of electrons located at a large effective distance from gate. From the futuristic point of view, our simulation results shows that the device designs of $Al_xGa_{1-x}N/GaN$ nanostructures HEMTs could be proposed for ultra-high speed logic amplifications of next-generation and high power switching applications fields in the future.

IV Conclusion and future work prospects

IV Conclusion and future work prospects

IV.1 General Conclusion

Due to its excellent material properties, GaN-based technology is set to become the dominant semiconductor in high-power and high-speed electronics. The research and development aimed at finding engineering solutions to gain the maximum potential from this material is gathering pace, and the work reported in this thesis is one of the many contributions to this goal. In this thesis, we have presented the results of the simulation of AlGaN/GaN HEMTs transistors and its performance for high frequency applications in order to manufacture high-performance components.

In the first chapter, we recalled the physical and electronic properties of the GaN material. This analysis showed the fundamental differences between this material and more conventional III-V semiconductors such as gallium arsenide. Its large forbidden energy band, its large direct gap which is 3.4 eV, its high saturation speed as well as its piezoelectric aspects make it an ideal candidate for high power microwave applications. Unlike other large-gap semiconductors such as silicon carbide or diamond, gallium nitride offers the possibility of producing ternary alloys such as AlGaN, InGaN or AlInN, which makes it possible to produce heterojunctions with high electronic mobility that can be used. for manufacturing faster field effect transistors. These properties allow HEMTs transistors to present better frequency performance.

In the second chapter, we have introduced the High Electron Mobility Transistors (HEMTs). Then, we studied the operating principle of the HEMT transistor based on AlGaN/GaN, its structure and the different layers that compose it and the different substrates choice such as Silicon Carbide Substrates (SiC), Sapphire Substrates (Al_2O_3) and Silicon Substrates (Si). The HEMTs on AlGaN/GaN heterostructure on sapphire substrate have shown desirable performances but due to poor thermal conductivity of sapphire substrate they are not suitable for high temperature and high power application. The suitability of AlGaN/GaN HEMTs on silicon substrates have been proved by RoundHEMT device.

In the third chapter, we modeled our device which is the HEMT AlGaN/GaN, we simulated and interpreted the different results. For this, we used the simulation software: MATLAB. We simulate the electrical characteristics of $Al_xGa_{1-x}N$/GaN nanostructures HEMTs by using samples with a different gate bias, different gate width, and with different thickness of $Al_xGa_{1-x}N$ barrier layer

and spacer layer, the study of the influence of the various geometrical parameters of the transistor on the electrical characteristics in order to obtain a structure conducive to good operation.

At the final point, our simulation results shows that the device designs of $Al_xGa_{1-x}N/GaN$ nanostructures HEMTs could be proposed for ultra-high speed logic amplifications of next-generation and high power switching applications fields in the future.

IV.2 Future work prospects

The prospects for this work turn to research into the performance of HEMTs for high voltage applications (voltage withstand, reduction of leakage currents, increase of the drain current) and the standardization of its performance on the whole of the epitaxial plate. However, further work on material growth, process technology, and device characterization, reliability and circuit integration is required in order for these devices to be considered for actual applications.

- Physical models should be developed to optimize material growth and enable the evaluation of new device structures by simulations. Furthermore, MOCVD growth of AlGaN/GaN epilayers on high-resistivity.
- The investigation of new device concepts such as an indium gallium nitride (InGaN) channel structure sandwiched between two GaN barrier layers and the double barrier AlGaN/GaN structure.
- To improve device performance and reliability, we recommend the development of drain and source contacts that show ohmic behavior either as deposited or after rapid thermal annealing at low temperatures, i.e. $T < 660\ ^oC$, which is the melting point of aluminum.
- In device characterization, accurate measurements should be done to enable the development of small and large signal transistor models that can be used to simulate device performance as a function of device layout.

Finally, reliability testing of GaN-based devices is an important topic to be addressed with respect to commercialization of this technology; it would be desirable to study the transistor even further, in search of better results. One could use the ternary AlInN which admits a better mesh agreement with GaN, and reduce the dimensions of the device to move towards “Nanotechnology”.

REFERENCES

Chapter I

1. Yoshikawa, A. “Development and Applications of Wide Bandgap Semiconductors”. In Yoshikawa, A.; Matsunami, H.; Nanishi, Y. (eds.). Wide Bandgap Semiconductors. Springer. p. 2, 2007.
2. Goyal, Nitin; Fjeldly, Tor A. “Effects of strain relaxation on bare surface barrier height and two-dimensional electron gas in AlxGa1-xN/GaN heterostructures.” Journal of Applied Physics. (ISSN 0021-8979). 113(1): 014505, 2013.
3. D.Neamen, An Introduction to Semiconductor Devices, 1st Ed. McGraw-Hill, USA (2006).
4. "NSM Archive - Physical Properties of Semiconductors". www.ioffe.ru. Archived from the original on 2015-09-28. Retrieved 2010-07-10.
5. Ahi, Kiarash (September 2017). "Review of GaN-based devices for terahertz operation". Optical Engineering. 56 (9): 090901.
6. Johnson et al. “Nitride Semiconductor Light-Emitting Diodes (LEDs) (Second Edition)”. Woodhead Publishing Series in Electronic and Optical Materials, Pages 3-23, 2018.
7. W. Seifert, R. Franzheld, E. Butter, H. Subotta, and V. Riede, “On the origin of free carriers in high-conducting n-GaN,” Crystal Res. and Technol., vol. 18, p. 383, 1983.
8. S. Nakamura, “In situ monitoring of GaN growth using interference effects,” Jpn. J. Appl. Phys., vol. 30, no. 8, pp. 1620–1627, Aug. 1991.
9. Stéphanie Anceau, « Etude des propriétés physiques des puits quantiques d’alliages quaternaires (Al,Ga,In) N pour la conception d’émetteurs ultraviolets », thèse de doctorat de l'université Montpellier , 2004.
10. J. L. Rouviere, M. Arlery, B. Daudin, G. Feuillet, et O. Briot, Material Science and Engineering B 50, 61 (1997).
11. Razeghi, Henini, « Optoelectronic Devices - III Nitrides », Elsevier, (2005).
12. M. Seelmann-Eggebert, J. L. Weyher, H. Obloh, H. Zimmermann, A. Rar, et S. Porowski, Appl. Phys. Lett. 71, 2635 (1997).

13. M. Leszczynski,J. Edgar, S. Strite, I. Akasaki, H. Amano and C. Wetzel,"Common crystal structure of the group III nitrides,Properties, processing and applications of gallium nitride and related semiconductors",1998, Publication INSPEC, Datareview series n°23, p3-5.
14. O. Brandt, "Cubic group III nitride, Group III nitride semiconductor compounds – physics and applications", 1998, B. GIL, Oxford Science Publication , p417-459.
15. Richard MEUNIER, M. Frédéric MORANCHO, "Optimization of the elaboration of insulating layers for the gate structures and the passivation of MIS-HEMT transistors on GaN." Doctorat de l'Université de Toulouse, p13, 22 juin 2016.
16. Krämer, Mark. C. J. C. M. (2006). "Gallium nitride-based microwave high-power heterostructure field-effect transistors." Technische Universiteit Eindhoven, pp.7-9, 01/01/2006.
17. ——, "LED breakthrough highlights AlN promise," Compound Semiconductor, vol. 12, no. 5, pp. 31–32, June 2006.
18. Krämer, Mark. C. J. C. M. (2006). "Gallium nitride-based microwave high-power heterostructure field-effect transistors." Technische Universiteit Eindhoven, pp.10-11, 01/01/2006.
19. M. Hatcher, "RFMD road-tests its 100 W GaN amplifiers," Compound Semiconductor, vol. 11, p. 13, June 2005.
20. "Non-led applications are set to bolster GaN sector," Compound Semiconductor, vol. 11, p. 10, May 2005.
21. "GaN Semiconductor Devices Market Size, Share & Trends Analysis Report." Grand View Research, pp.182, Sep, 2020.
22. Richard Eden, "GaN & SiC power semiconductor markets set to pass $1 billion mark in 2021." Omdia informa tech, 22 Jul 2020.
23. Sophie Barbet, « Etude par microscopie à champ proche de matériaux III-N pour émetteurs électriques planaires », thèse doctorat, Université des sciences et technologies de Lille (2008).
24. I. Akasaki, H. Amano, and S. Nakamura, "Nobel Prize in Physics: Invention of efficient blue light-emitting diodes." Nobel Foundation, October 7, 2014.
25. C.-L. Hsiao, J. Palisaitis, M. Junaid, P.O.Å. Persson, J. Jensen, Q.-X. Zhao, L. Hultman, L.-C. Chen, K.-H. Chen, and J. Birch, "Room- temperature heteroepitaxy of single-phase

Al1−xInxN films with full composition range on isostructural wurtzite templates", Thin Solid Films 524, 113 (2012).

26. O. Ambacher et al. "Two-dimensional electron gases induced by spontaneous and piezoelectric polarization charges in N- and Ga-face AlGaN/GaN heterostructures" , J. Appl. Phys. – 1999.– V. 85.– P. 3222–3233.
27. Richard MEUNIER, "Optimization of the elaboration of insulating layers for the gate structures and the passivation of MIS-HEMT transistors on GaN : GaN for power electronics." Doctorat de l'Université de Toulouse, pp.20, 22 juin 2016.

Chapter II

1. Sheppard, S.; Doverspike, K.; Pribble,W.; Allen, S.; Palmour, J.; Kehias, L.; Jenkins, T. High-power microwave GaN/AlGaN HEMTs on semi-insulating silicon carbide substrates. IEEE Electron. Device Lett. 1999, 20, 161–163.
2. Strite, S.; Morkoç, H. GaN, AlN, and InN: A review. J. Vac. Sci. Technol. B 1992, 10, 1237.
3. R. Dingle ; H.L. Stormer ; A.C. Gossard ; and W. Wiegmann « Electron mobilities in modulation-doped semiconductor heterojunction superlattices» Applied Physics Letters, vol. 33, no. 7, pp. 665–667, 1978.
4. C. Charbonniaud, T. Gasseling, S. De Meyer, R. Quéré, J.P. Teyssier, D. Barataud, J.M Nébus, T.Martin, B. Grimbert, V. Hoel, N. Caillas, E. Morvan, « Power Performance Evaluation of AlGaN/GaN HEMTs through Load Pull and Pulsed I-V Measurements», GAAS 2004, 11-12 Oct, 2004 Amsterdam.
5. A. Chini, D. Buttari, R. Coffie, S. Heikman, S. Keller ; U.K. Mishra, «12W/mm power density AlGaN/GaN HEMTs on sapphire substrate», Electronics Letters, Vol. 40, No 1, January 2004.
6. Z. Oussama, « Étude et caractérisation d'un microsystème à base de matériau nitruré AlGaN pour les applications biologique et biomédicale. » Thèse de doctorat Université de Tlemcen, pp.48 ,15/03/2015.
7. S. De Mayer « Etude d'une nouvelle filière de composants HEMTs sur technologie nitrure de gallium. Conception d'une architecture flip-chip d'amplificateur distribué de puissance à très large bande », Thèse de doctorat, Université de Limoges, 2005.

8. J.W. Johnson, E.L.Piner, A. Vescan, R.Therrien,P. Rajagopal, J.C. Roberts,J.D. Brown, S. Singhal, and K.J. Linthicum. 12 W/mm AlGaN-GaN HFETs on silicon substrates. IEEE Electron Device Letters (2004) 25: p. 459.
9. M. Ruff, H. Mitlehner and R. Helbig, "SiC devices: physics and numerical simulation", *IEEE Transactions on Electron Devices*, vol. 41, pp. 1040-1054, Jun 1994.
10. L. Liu, J.H. Edgar. Substrates for Gallium Nitride epitaxy.Materials Science and Engineering, R37, pp 112, 2002.
11. S. Boeykens et al., « Investigation of AlN nucleation layers for AlGaN/GaN heterostructures on 4H-SiC » phys. stat. sol. (c) 3, No. 6, 1579–1582 (2006).
12. H. Liu, W. So, K. Ma, B.Yuan, C. Chern. nHigh volume AlInGaN LED manufacturing at AXT.Compound Semi-Conductor. Vol 7. No. 10, pp 59-61, Novembre 2001.
13. Z. Oussama, « Étude et caractérisation d'un microsystème à base de matériau nitruré AlGaN pour les applications biologique et biomédicale. » Thèse de doctorat Université de Tlemcen, pp.24-25 ,15/03/2015.
14. Douglas, E.A.; Chang, C.Y.; Cheney, D.J. AlGaN/GaN High Electron Mobility Transistor degradation under on- and off-state stress. Microelectron. Reliab. 2011, 51, 207–211.
15. Joh, J.; Alamo, J.A.D. A Current-Transient Methodology for Trap Analysis for GaN High Electron Mobility Transistors. IEEE Trans. Electron Devices 2011, 58, 132–140.
16. Makaram, P.; Joh, J.; Jesús, A.D.A. Evolution of structural defects associated with electrical degradation in AlGaN/GaN high electron mobility transistors. Appl. Phys. Lett. 2010, 96, 756–758.
17. Chang, Y.; Tong, K.Y.; Surya, C. Numerical simulation of current–voltage characteristics of AlGaN/GaN HEMTs at high temperatures. Semicond. Sci. Technol. 2015, 20, 188–192.

Chapter III

1. J. C. Freeman, "Basic equations for the modeling of gallium nitride (GaN) high electron mobility transistors (HEMTs)," NASA Report NASA/TM-2003-211983, 2003.
2. M. Gerritsen, "A brief introduction to MATLAB." Linear Algebra with Application to Engineering Computations, pp.2, September 2006.
3. The MathWorks Inc. MATLAB 7.0 (R14SP2). The MathWorks Inc., 2005.

4. David Houcque, “Introdution to Matlab for engineering students.” Northwestern University, pp.1, version 1.2, August 2005.
5. D. Delegebeaudeuf and N. T. Linh, “Metal-(n)AlGaAs-GaAs two dimensional electron gas FET,” IEEE Electron Device Lett., vol. 29, no. 6, pp. 955–960, Jun. 1982.
6. S. Kola, J. M. Golio, and G. N. Maracas, “An analytical expression for Fermi level versus carrier concentration for HEMT modeling,” IEEE Electron Device Lett., vol. 9, no. 3, pp. 136–138, Mar. 1988.
7. K. Lee, M. Shur, T. J. Drummond, and H. Morkoc, “Current-voltage and capacitance-voltage characteristics of modulation doped field-effect transistors,” IEEE Trans. Electron Devices, vol. 30, no. 3, pp. 207–212, Mar. 1983.
8. S. Khandelwal, N. Goyal, and T. A. Fjeldly, “A physics based analytical model for 2DEG charge density in AlGaN/GaN HEMT devices,” IEEE Trans. Electron Devices, vol. 58, no. 10, pp. 3622–3625, Oct. 2011.
9. S. Khandelwal and T. A. Fjeldly, “A physics based compact model for I–V and C–V characteristics in AlGaN/GaN HEMT devices,” Solid State Electron., vol. 76, pp. 60–66, Oct. 2012.
10. F. Lime, B. Iniguez, and O. Moldovan, “A quasi-two-dimensional compact drain-current model for undoped symmetric double-gate MOSFETs including short-channel effects,” IEEE Trans. Electron Devices, vol. 55, no. 6, pp. 1441–1448, Jun. 2008.
11. B. Iñiguez and E. Garcia-Moreno, “An improved C∞-continuous smallgeometry MOSFET modeling for analog applications,” Analog Integr. Circuits, Signal Process., vol. 13, no. 3, pp. 241–259, Jul. 1997.
12. T. Ytterdal, Y. Cheng, and T. A. Fjeldly, Device Modeling for Analog and RF Circuit Design. New York, NY, USA: Wiley, 2003, pp. 31–36.
13. X. Cheng and Y. Wang, “A surface-potential-based compact model for AlGaN/GaN MODFETs,” IEEE Trans. Electron Devices, vol. 58, no. 2, pp. 448–454, Feb. 2011.
14. X. Cheng, M. Li, and Y. Wang, “An analytical model for currentvoltage characteristics of AlGaN/GaN HEMTs in presence of selfheating effect,” Solid State Electron., vol. 54, no. 1, pp. 42–47, Jan. 2010.
15. Li. Yuan, Hongwei. Chen, Kevin.J. Chen, "Normally Off AlGaN/GaN Metal-2DEG Tunnel-Junction Field-Effect Transistors", IEEE electron device letters , Vol. 32, N°.3, pp.303-305, March 2011.

16. E. Tschumak, R. Granzner, J.K.N. Lindner, F. Schwierz, K. Lischka, H. Nagasawa, M. Abe, D.J. As, "Non-polar Cubic AlxGa1-xN/GaN Hetero-Junction Field Effect Transistor on Ar+ Implanted 3C-SiC (001)", Appl, Phys, Lett., Vol. 96, pp.253-501, June 2010.